SAND2017-7334C

Exceptional service in the national interest

Sandia National Laboratories

Dislocation-based approaches for simulating plastic deformation in BCC metals under high-rate loading

C.C. Battaile[1], H. Lim[1], J.D. Carroll[1], and C.R. Weinberger[2]

[1] Sandia National Laboratories
[2] Colorado State University

International Symposium on Plasticity
January 3 2017

U.S. DEPARTMENT OF ENERGY

NNSA National Nuclear Security Administration

Sandia National Laboratories is a multi-program laboratory managed and operated by Sandia Corporation, a wholly owned subsidiary of Lockheed Martin Corporation, for the U.S. Department of Energy's National Nuclear Security Administration under contract DE-AC04-94AL85000.

Dislocation Plasticity in BCC Metals

BCC metals deform via the propagation of screw dislocations, whose atomic structure is complex. Dislocation cores "spread" onto multiple crystallographic planes.

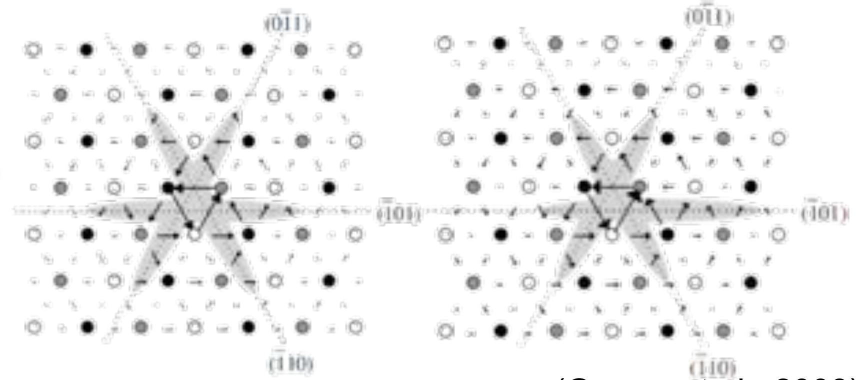

(Groger et al., 2008)

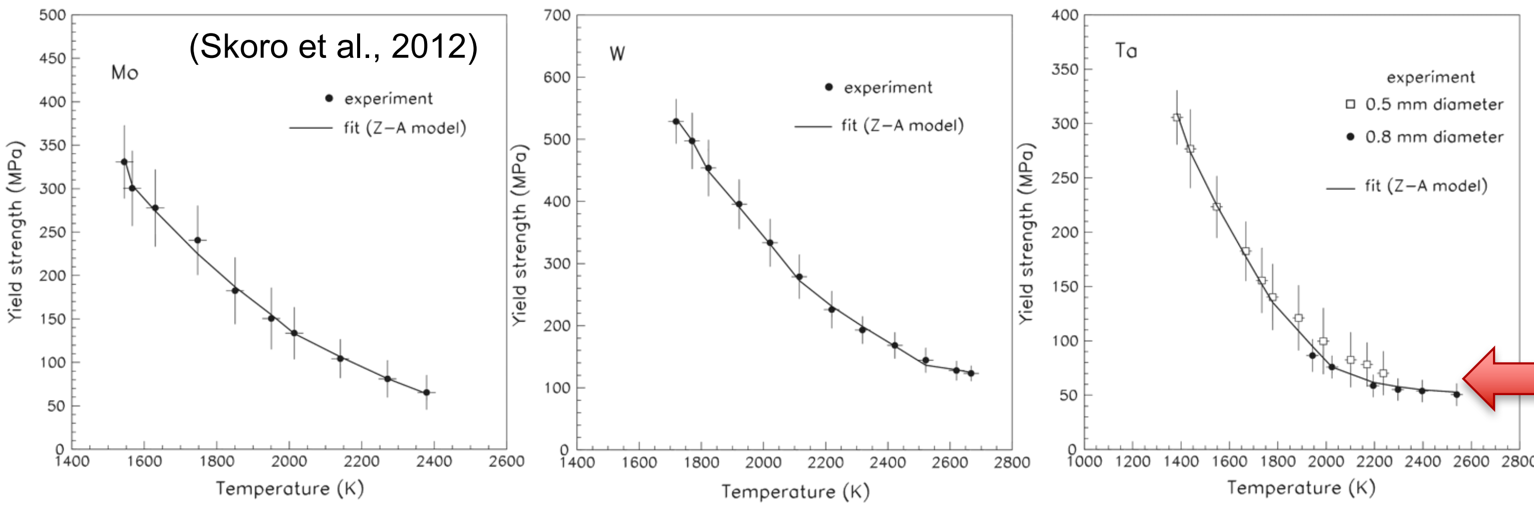

Therefore, BCC metals' strength is strongly dependent on T (and $\dot{\epsilon}$).

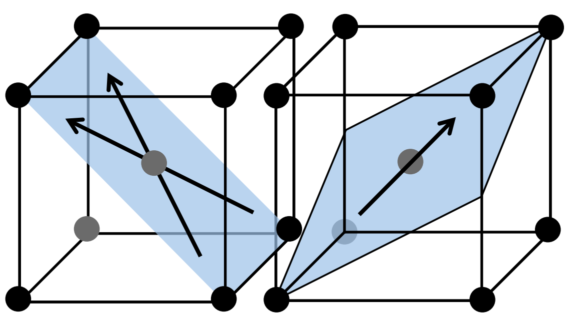

{110} slip {112} slip

$$\tau(T,\dot{\gamma}) = \underbrace{\tau^{*}(T,\dot{\gamma})}_{\text{Thermal}} + \underbrace{\tau_{obs}}_{\text{Athermal}}$$

In FCC metals, $\tau^{*} \approx 0$

In BCC metals, $\tau^{*} >> 0 \ (T << T_c)$

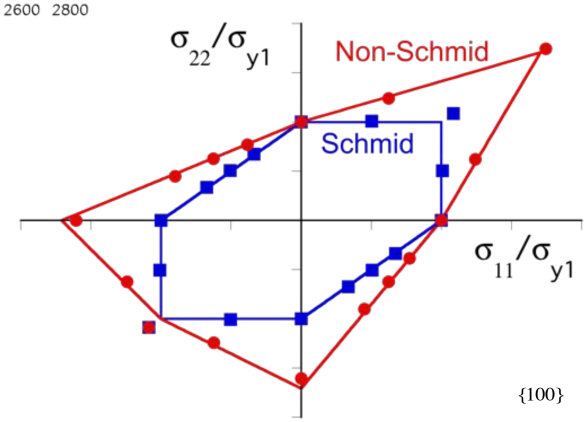

Multi-scale Modeling of BCC Metals

Atomic scale phenomena	Single crystal behavior	Validation	Polycrystal behavior	Continuum response

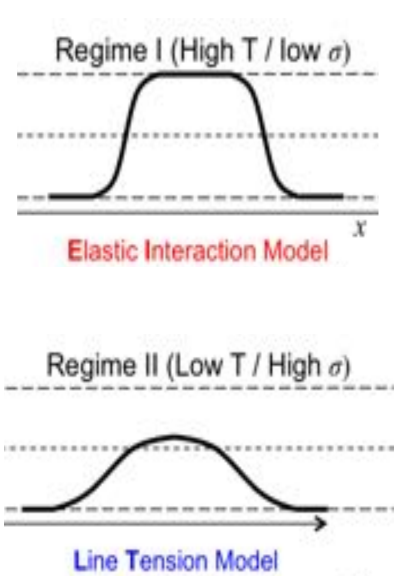

Dislocation kink-pair theory

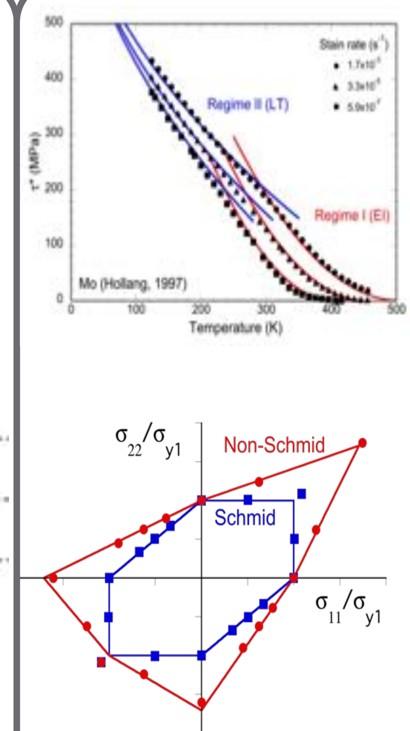

Single crystal constitutive model

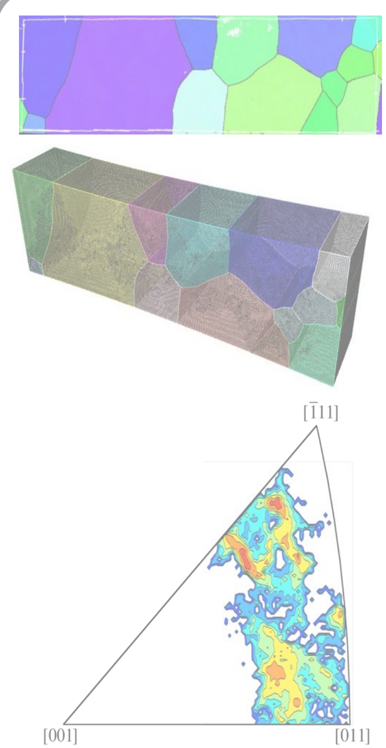

Compare with experiments

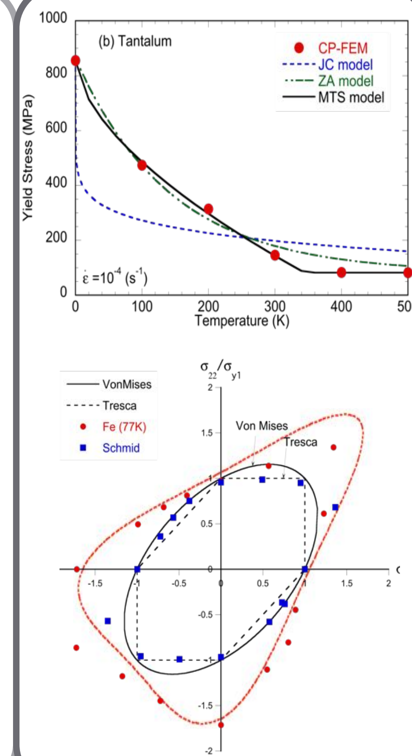

Bulk strength model

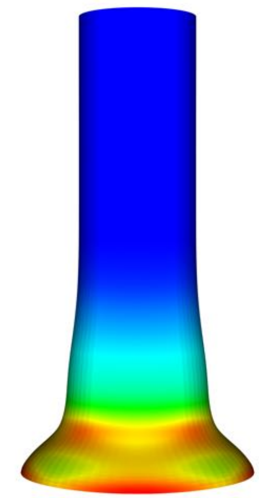

Simulations of impact tests

Dislocation Kink-Pair Theory

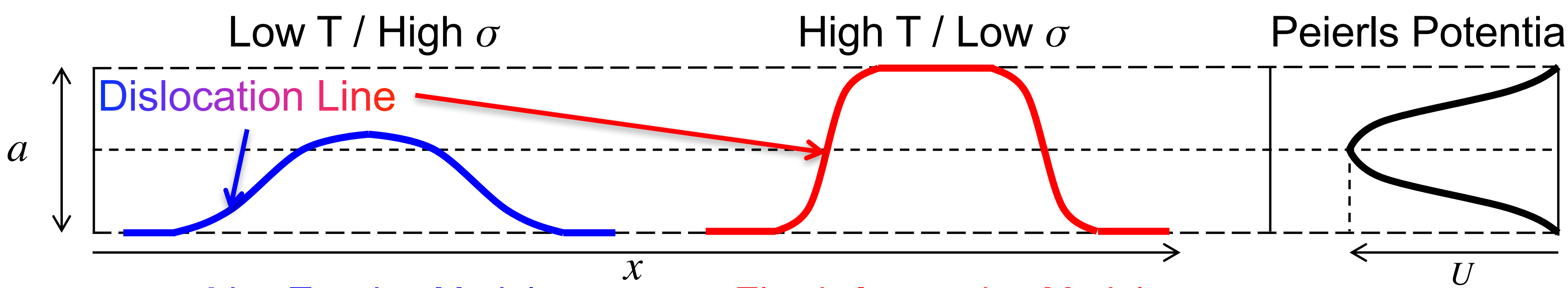

Line Tension Model

$$\tau^*_{LT}(T,\dot{\gamma}) = \tau^0_{LT}\left(1-\left(\frac{T}{T_c(\dot{\gamma})}\right)^{1/2}\right)$$

Elastic Interaction Model

$$\tau^*_{EI}(T,\dot{\gamma}) = \tau^0_{EI}\left(1-\frac{T}{T_c(\dot{\gamma})}\right)^{2}$$

$$T_c(\dot{\gamma}) = \frac{2H_k}{k_B \ln\left(\dot{\gamma}_0/\dot{\gamma}\right)}$$

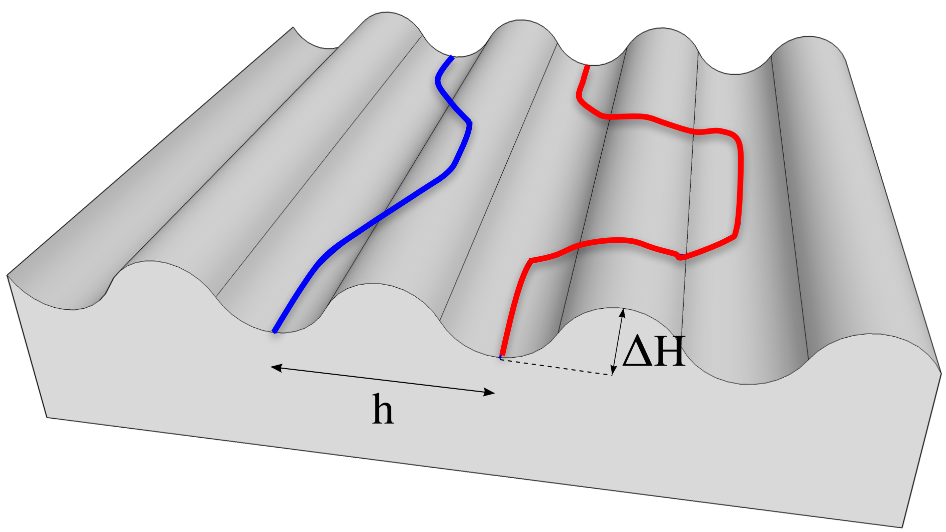

Best-fit material parameters

Material	$\dot{\gamma}_0\ (s^{-1})$	$2H_k\ (eV)$	$\tau^0_{EI}\ (MPa)$	$\tau^0_{LT}\ (MPa)$
Mo	3.75×10^{9}	1.27	1156	835
Ta	2.99×10^{6}	0.85	406	320
W	3.71×10^{10}	2.06	2035	1038
Nb	1.14×10^{8}	0.68	576	402

Calibration / Validation of KP Theory

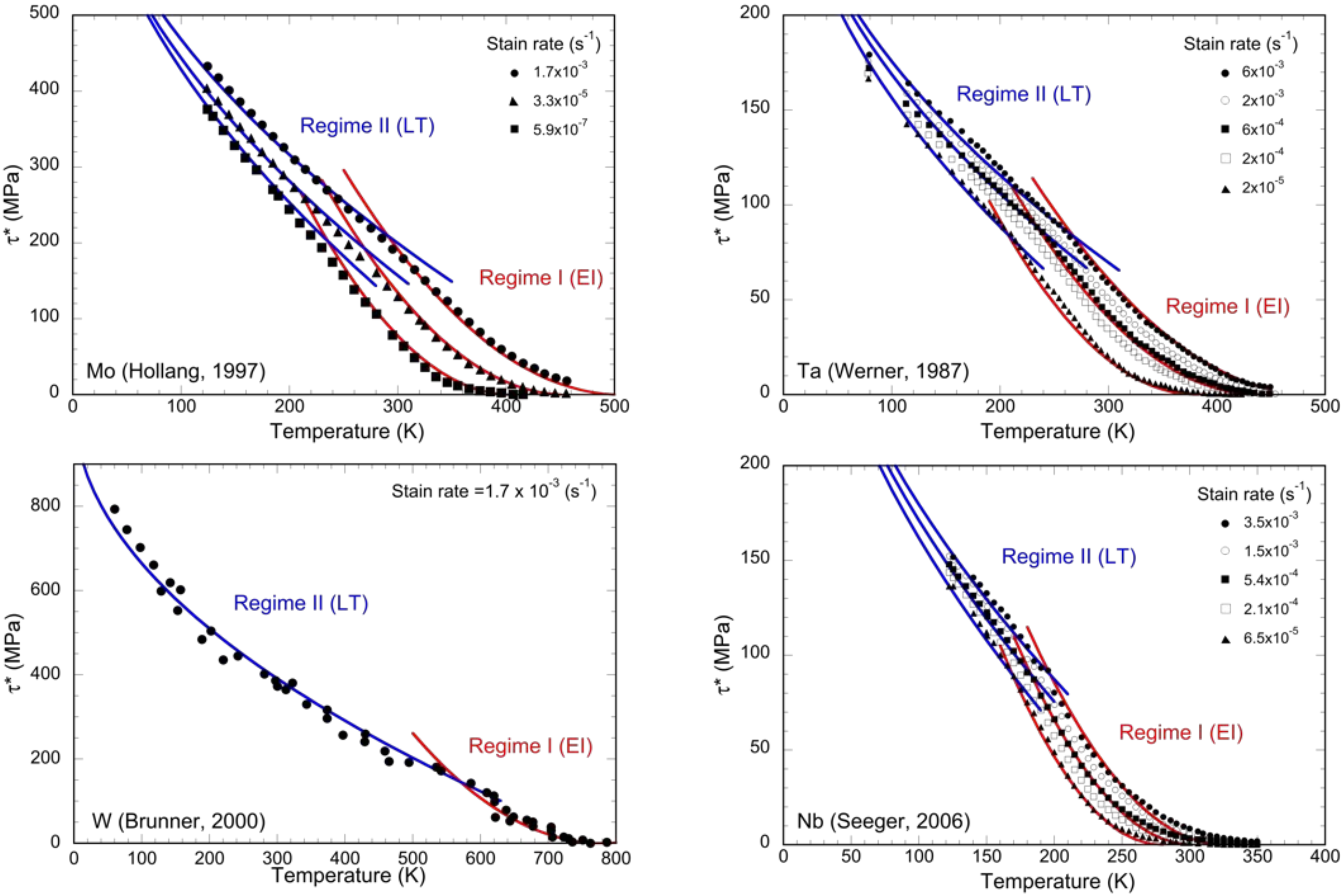

Measured τ^* are accurately reproduced by the EI and LT models

Crystal Plasticity Finite Element Model

- FEM code developed at Sandia National Laboratories (JAS-3D)
- 24 {110}<111> slip systems
- Slip rate: $\dot{\gamma}^{\alpha} = \dot{\gamma}_0^{\alpha} \left(\frac{\tau^{\alpha}}{g^{\alpha}} \right)^{1/m}$ (Hutchinson, 1976)
- Slip resistance: $g^{\alpha} = \min\left(\tau_{EI}^{*\alpha}, \tau_{LT}^{*\alpha} \right) + \tau_{obs}^{\alpha}$

$\tau_{EI}^{*\alpha}$ → Lattice friction; τ_{obs}^{α} → Obstacle stress

$$\tau_{EI}^{*}(T, \dot{\gamma}) = \tau_{EI}^{0} \left(1 - \frac{T}{T_c(\dot{\gamma})} \right)^{2}$$

$$\tau_{LT}^{*}(T, \dot{\gamma}) = \tau_{LT}^{0} \left(1 - \left(\frac{T}{T_c(\dot{\gamma})} \right)^{1/2} \right)$$

- Obstacle stress: $\tau_{obs}^{\alpha} = A\mu b \sqrt{\sum_{\beta=1}^{NS} \rho^{\beta}}$ (Taylor, 1934)

$$\dot{\rho}^{\alpha} = \left(\kappa_1 \sqrt{\sum_{\beta=1}^{NS} \rho^{\beta}} - \kappa_2 \rho^{\alpha} \right) \cdot \left| \dot{\gamma}^{\alpha} \right|$$ (Kocks, 1976)

More Details on Crystal Plasticity FEA

Cauchy stress resolved on each of 24 slip systems: $\tau = \mathbf{P}_s : \sigma \qquad \mathbf{P}_s = \frac{1}{2}(\mathbf{m} \otimes \mathbf{s} + \mathbf{s} \otimes \mathbf{m})$

Non-Schmid stress: $\tau_{ns} = \mathbf{P}_{ns} : \sigma \qquad \mathbf{P}_{ns} = c_1 \mathbf{m} \otimes \mathbf{t} + c_2 \mathbf{s} \otimes \mathbf{t} + c_3 \mathbf{s} \otimes \mathbf{s} + c_4 \mathbf{t} \otimes \mathbf{t} + c_5 \mathbf{m} \otimes \mathbf{m}$

Slip resistance ("hardness"): $g = \max(\tau_{cr} - \tau_{ns}, 0) + \tau_{obs}$

Slip rate on each system: $\dot{\gamma} = \dot{\gamma}_0 \left| \frac{\tau}{g} \right|^{\frac{1}{m}} sign(\tau)$

Plastic velocity gradient: $\hat{\mathbf{L}}_p = \dot{\gamma}(\hat{\mathbf{s}} \otimes \hat{\mathbf{m}})$

Plastic deformation gradient: (Cayley-Hamilton theorem)

$$\dot{\mathbf{F}}_p = \hat{\mathbf{L}}_p \bullet \mathbf{F}_p \Rightarrow \begin{cases} \mathbf{F}_p = \exp(\hat{\mathbf{L}}_p \Delta t)\mathbf{F}_p \\ \exp(\hat{\mathbf{L}}_p \Delta t) = I + \frac{\sin\phi}{\phi}\hat{\mathbf{L}}_p \Delta t + \frac{1-\cos\phi}{\phi^2}(\hat{\mathbf{L}}_p \bullet \hat{\mathbf{L}}_p)\Delta t^2 \\ \phi = \Delta t \sqrt{\frac{1}{2}(\hat{\mathbf{L}}_p : \hat{\mathbf{L}}_p)} \end{cases}$$

Elastic deformation gradient and strain: $\mathbf{F}_e = \mathbf{F} \bullet (\mathbf{F}_p)^{-1} \Rightarrow \hat{\mathbf{E}}_e = \frac{1}{2}\left[(\mathbf{F}_e)^T \bullet \mathbf{F}_e - \mathbf{I}\right]$

2nd Piola-Kirchhoff stress (hyper-elasticity): $\hat{\sigma}_{PK2} = \mathbf{C} : \hat{\mathbf{E}}_e$

Updated Cauchy stress: $\sigma = \frac{1}{J^{\mathbf{F}_e}}\left[\mathbf{F}_e \bullet \hat{\sigma}_{PK2} \bullet (\mathbf{F}_e)^T\right]$

Updated crystallographic orientation: $\mathbf{F}_e = \mathbf{U}_e \bullet \mathbf{R}_e \Rightarrow \mathbf{R}_{lattice} = \mathbf{R}_e \bullet \mathbf{R}_h$

Updated hardness: $\tau_{obs} = \alpha\mu b \sqrt{\sum_{\beta=1}^{NS} \rho^\beta} \qquad d\rho = \left(\kappa_1 \sqrt{\sum_{\beta=1}^{NS} \rho^\beta} - \kappa_2 \rho\right) \cdot |d\gamma|$

Single Crystal CP-FEM Predictions

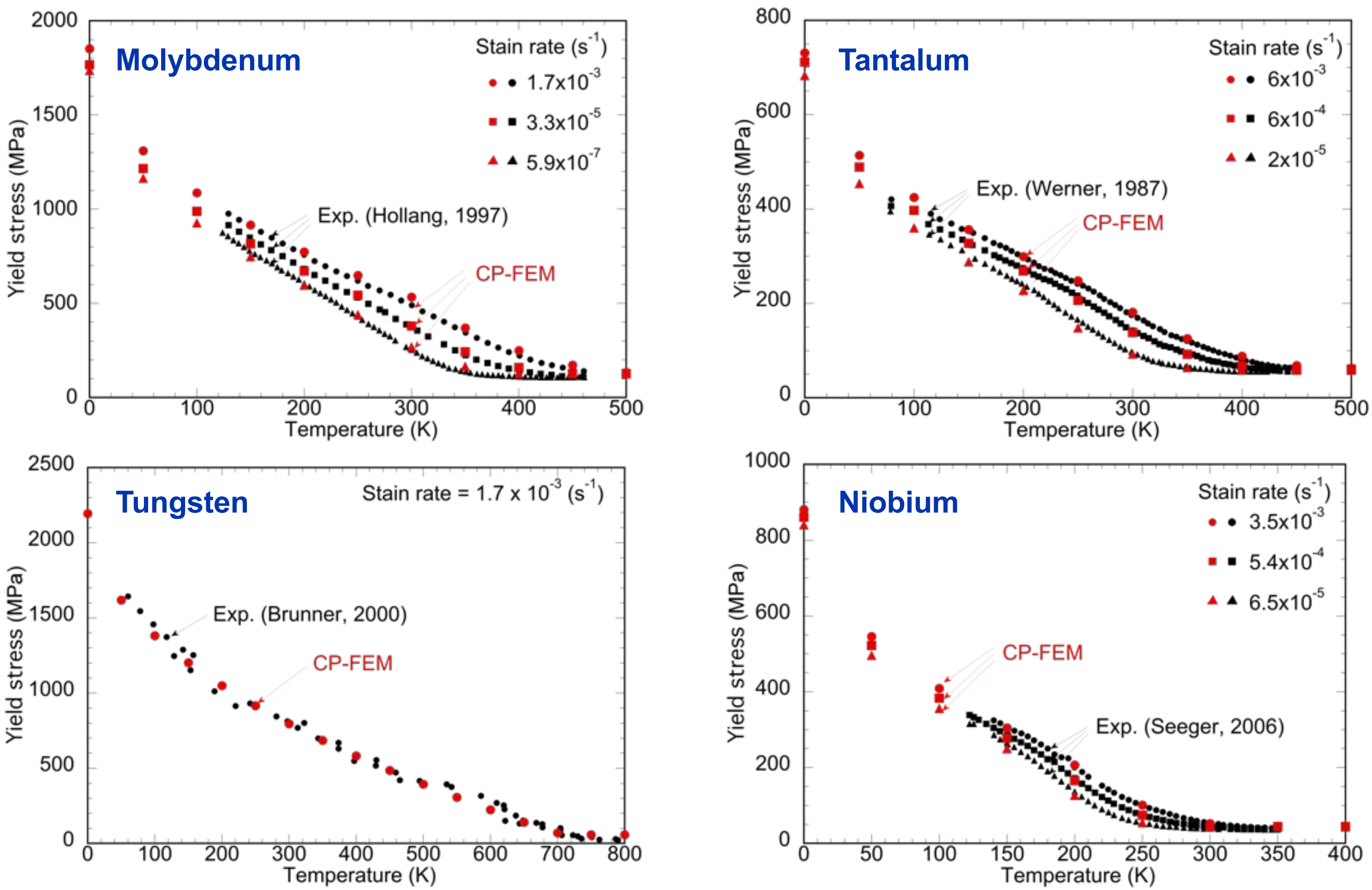

CP-FEM model accurately reproduced yield stresses of [$\bar{1}$49] single crystals

Polycrystal CP-FEM Predictions

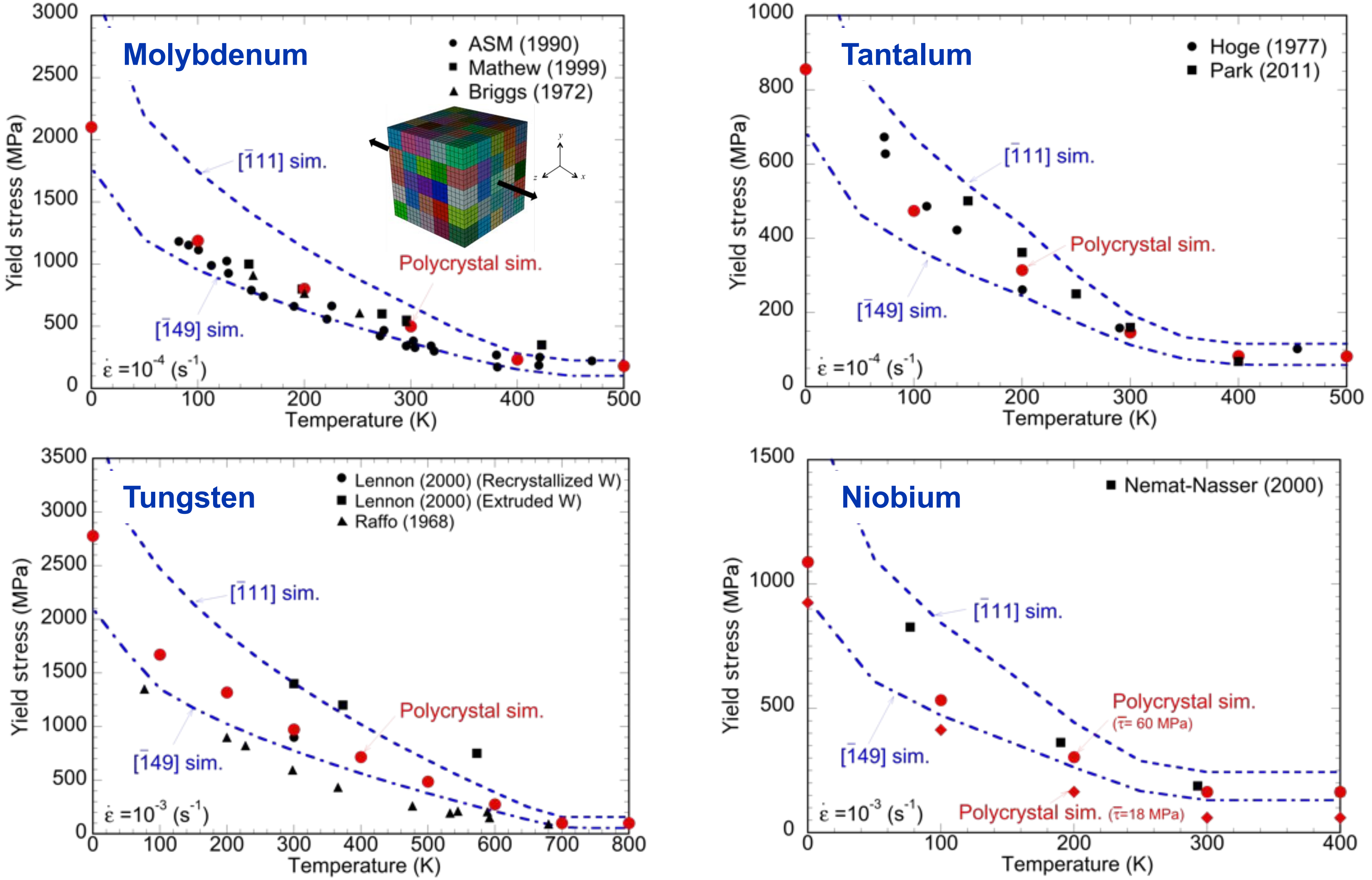

Measured yield stresses of BCC polycrystals lie between the bounds predicted by CP-FEM models on extreme single crystal orientation.

Polycrystal CP-FEM Predictions

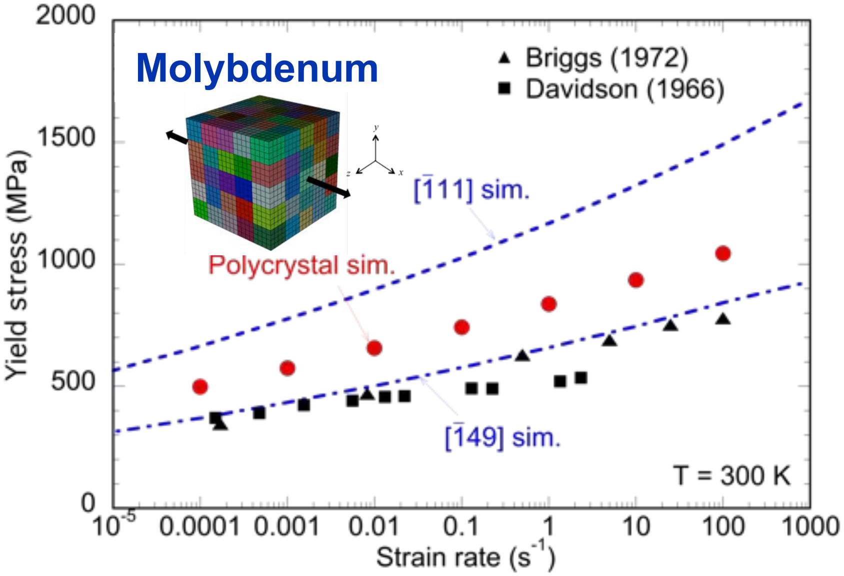

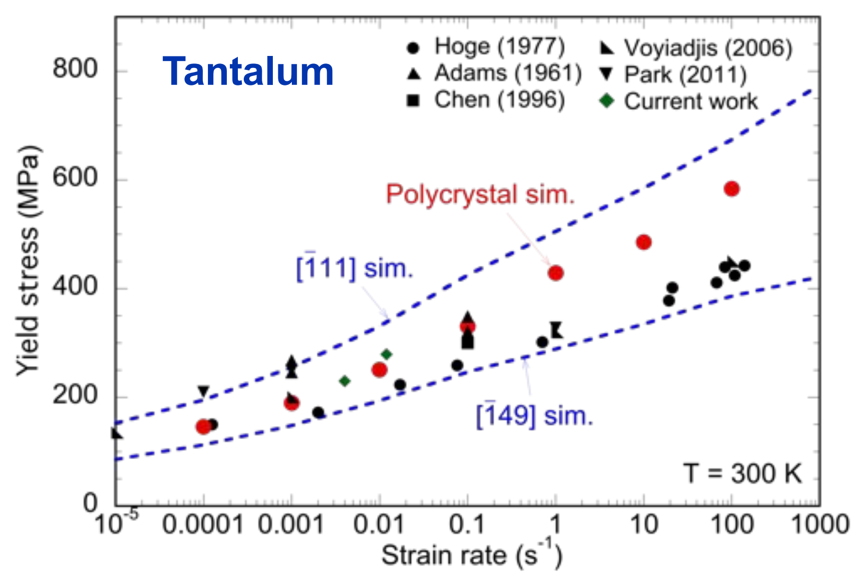

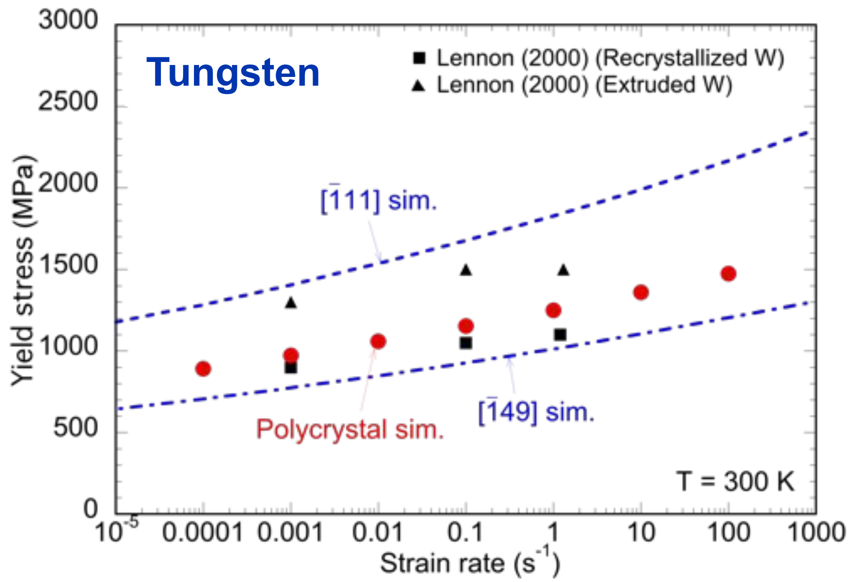

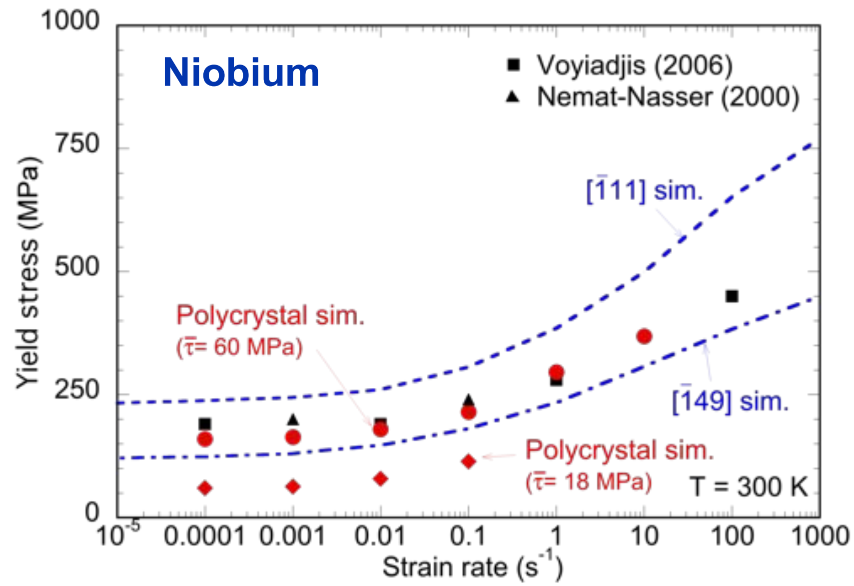

Measured yield stresses of BCC polycrystals lie between the bounds predicted by CP-FEM models on extreme single crystal orientation.

Continuum Constitutive Models

- Johnson and Cook (JC) model (Johnson and Cook, 1983, 1985)

$$\sigma_y^{JC} = A\left(1 + C\ln\dot{\varepsilon}\right)\left(1 - T^{*m}\right)$$

- Zerilli-Armstrong (ZA) model (Zerilli and Armstrong, 1987)

$$\sigma_y^{ZA} = C_0 + C_1\exp\left(-C_3T + C_4T\ln\dot{\varepsilon}\right)$$

- Mechanical Threshold Stress (MTS) model (Follansbee, 1988)

$$\sigma_y^{MTS} = \sigma_0 + \hat{\sigma}\left(1 - \left(\frac{k_B T}{G_0}\ln\frac{\dot{\varepsilon}}{\dot{\varepsilon}_0}\right)^{1/q}\right)^{1/p}$$

Continuum Constitutive Model Calibration

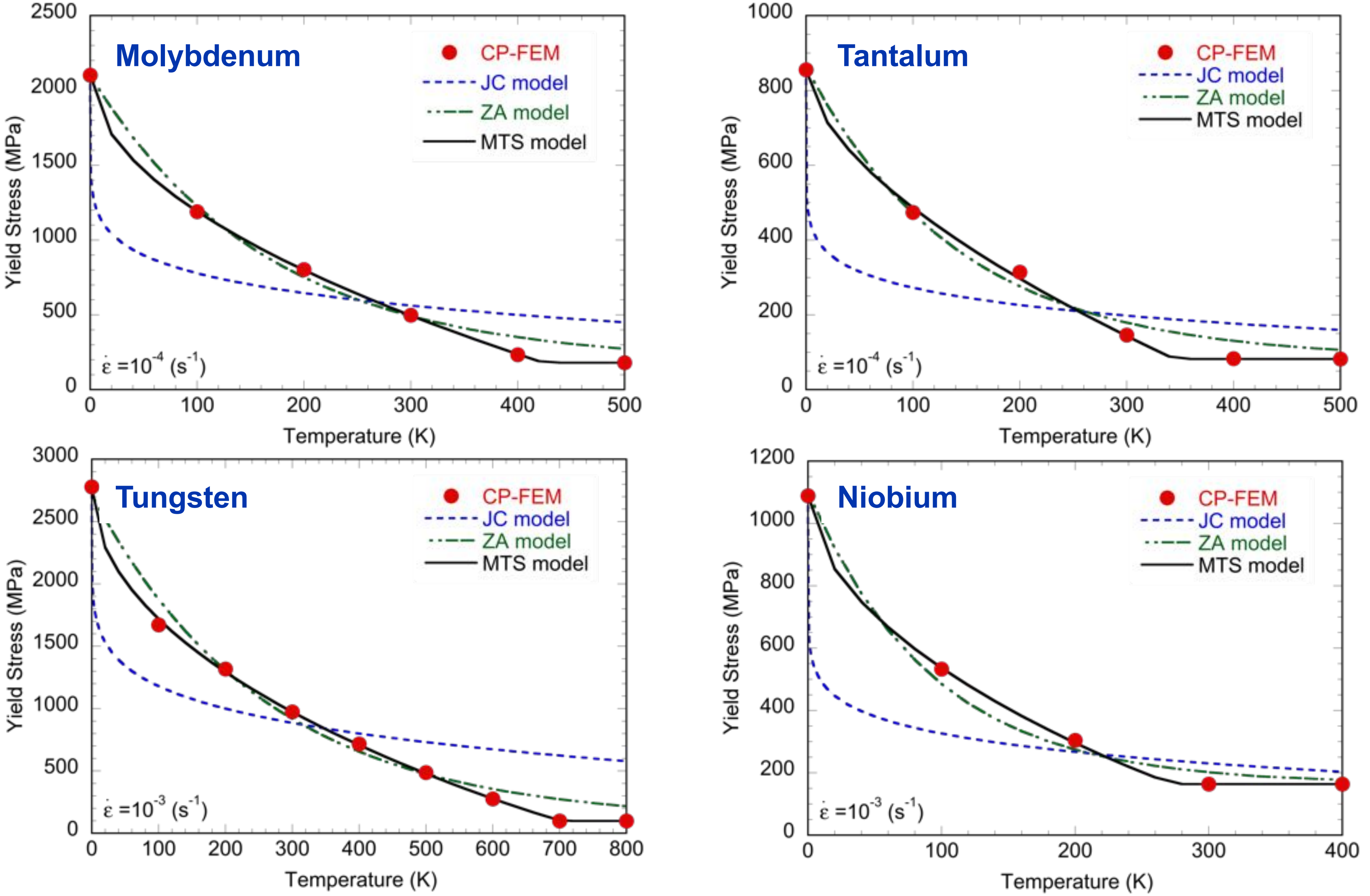

Continuum Constitutive Model Calibration

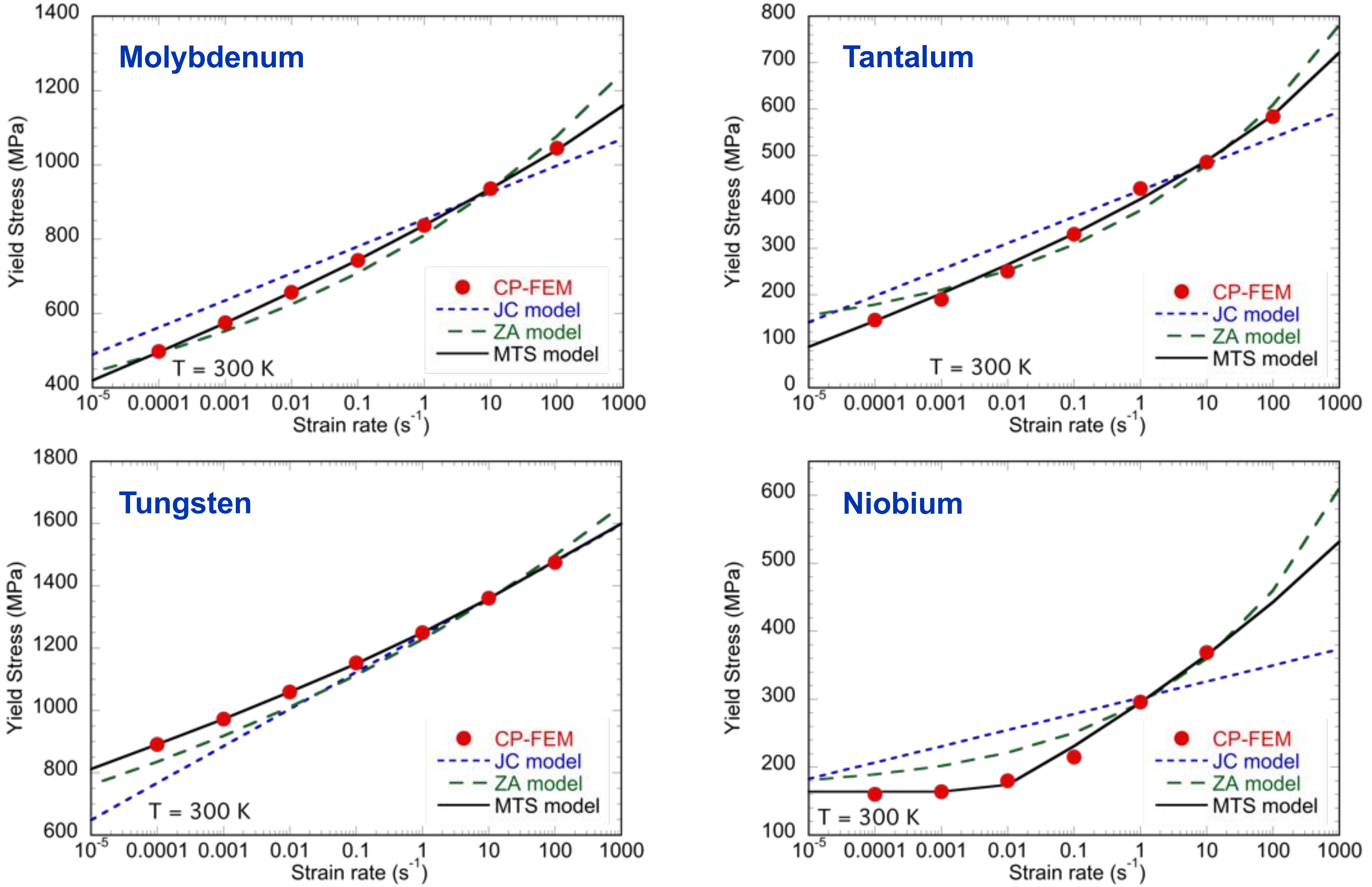

Simulations of Taylor Cylinder Impact Tests

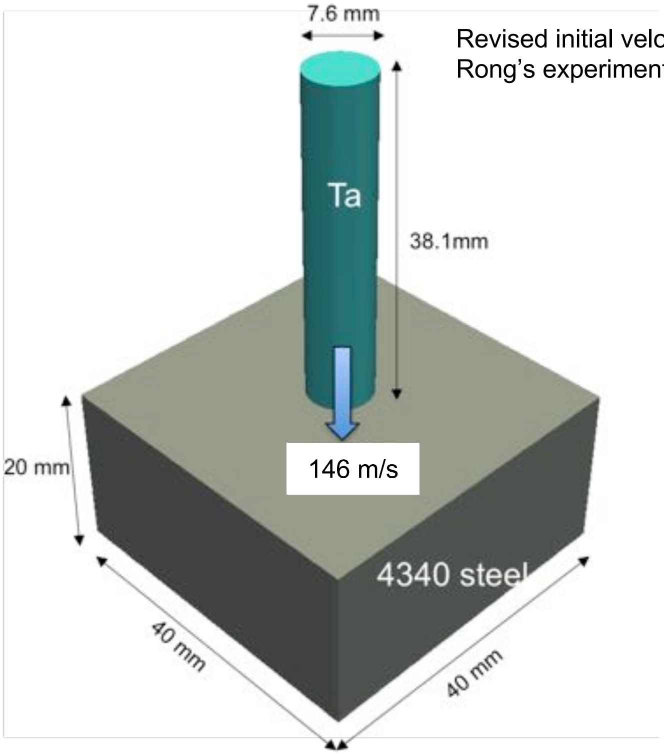

Revised initial velocity based on Shuh Rong's experimental measurements.

- Lagrangian
- Initial temperature = 298 K

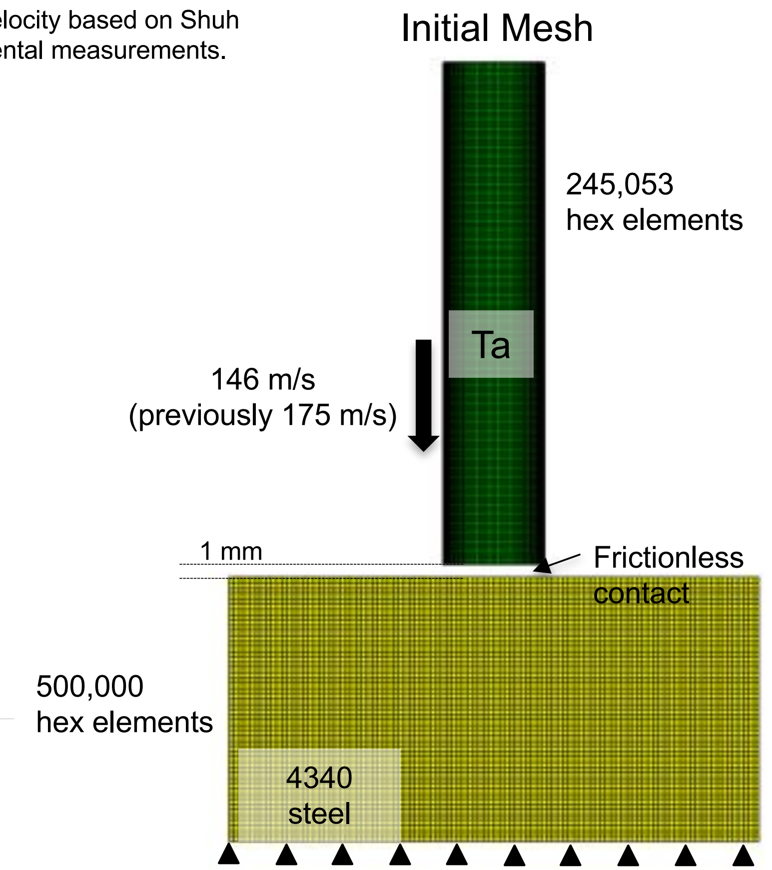

Simulations of Ta Taylor Cylinder Impact

38.1 x 7.62 mm
(.30 caliber)

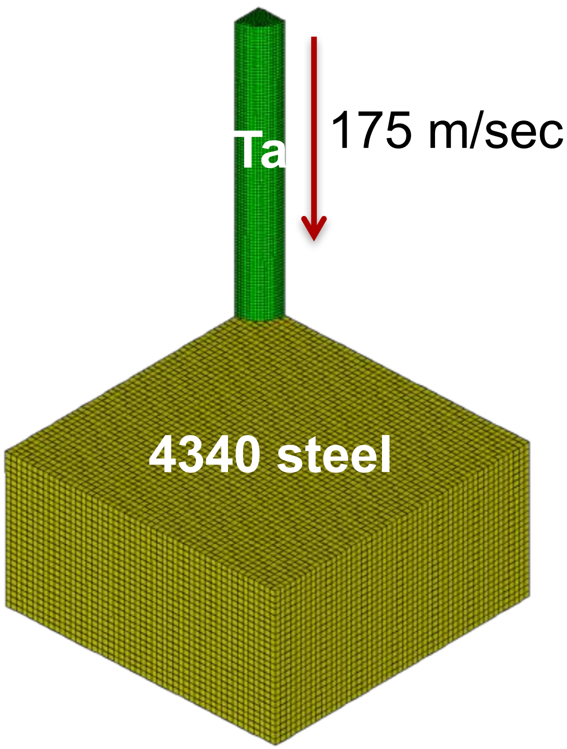

FE Mesh

Impact Simulation Results

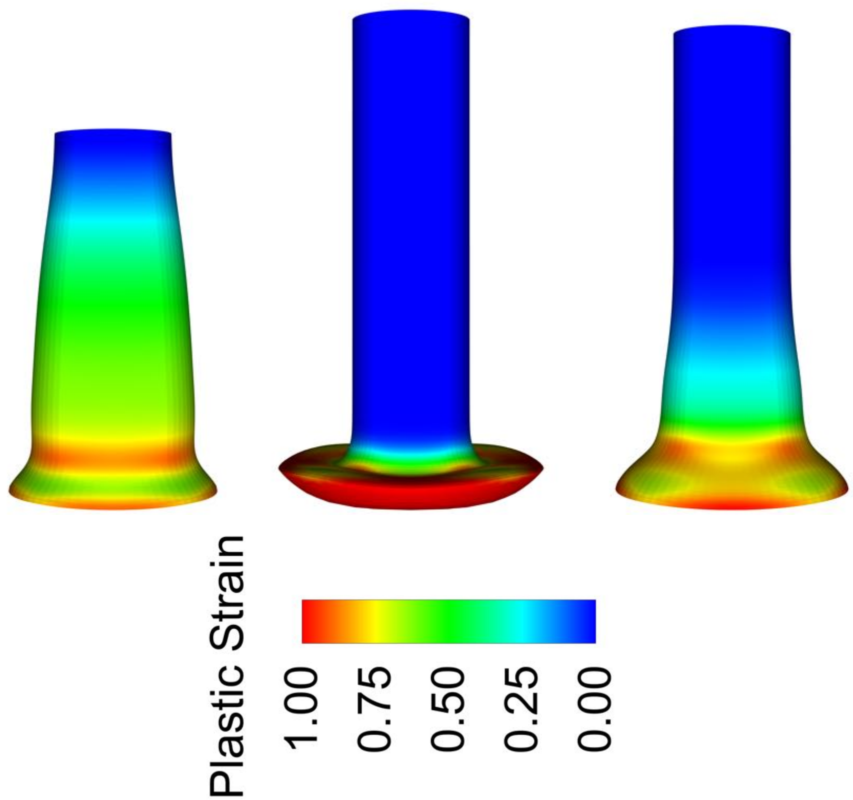

Experiment

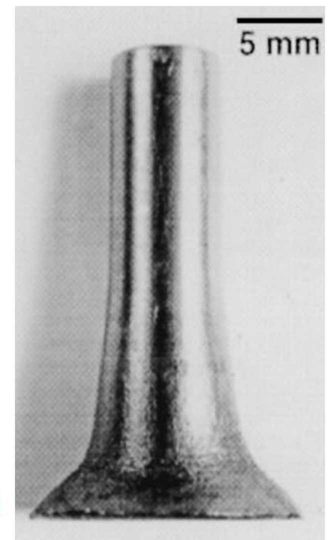

(Maudlin 1999)

Validation of Ta Taylor Cylinder Impact

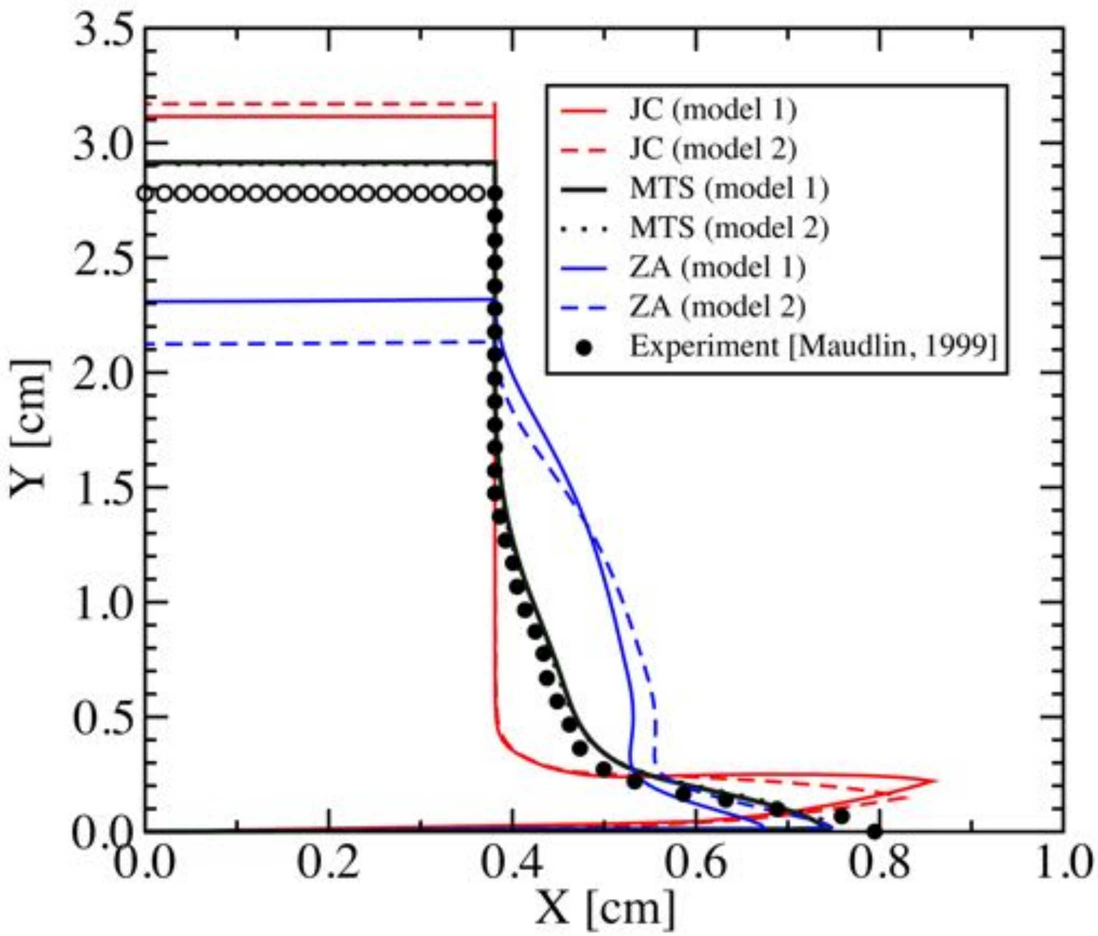

Deformed Projectile Shape

Strength Model Predictions at Higher Strain Rates

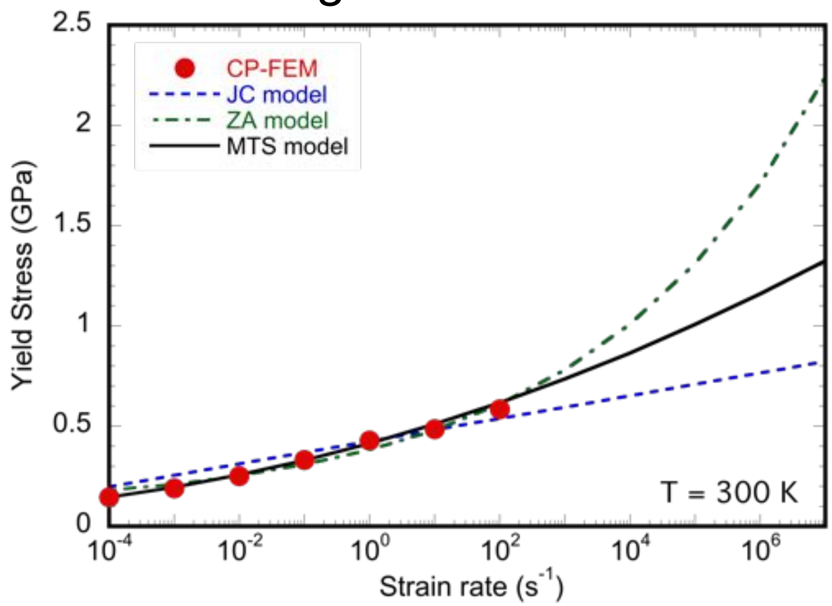

V = 146 m/s vs. 175 m/s

V = 146 m/s
HC Starck Ta

V = 175 m/s
DoD/DOE Ta

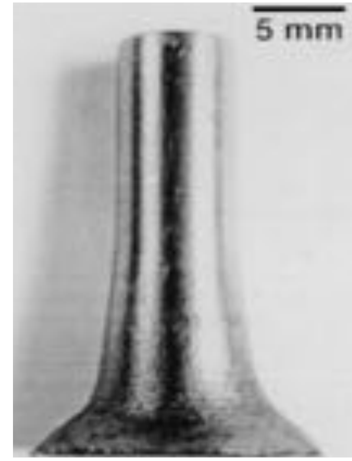

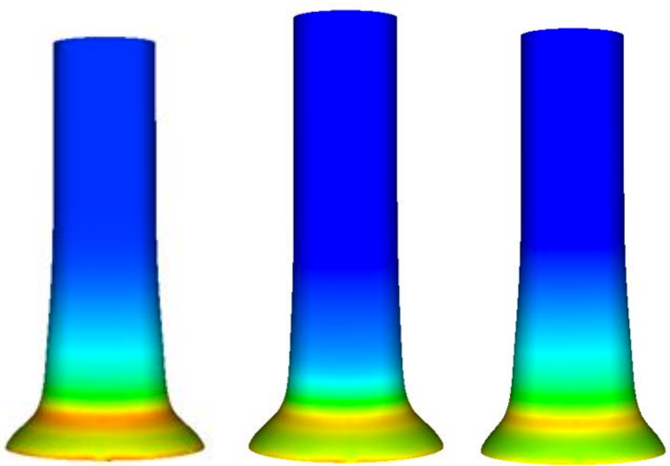

LANL's PTW model | Sandia's PTW model | Sandia's KP model

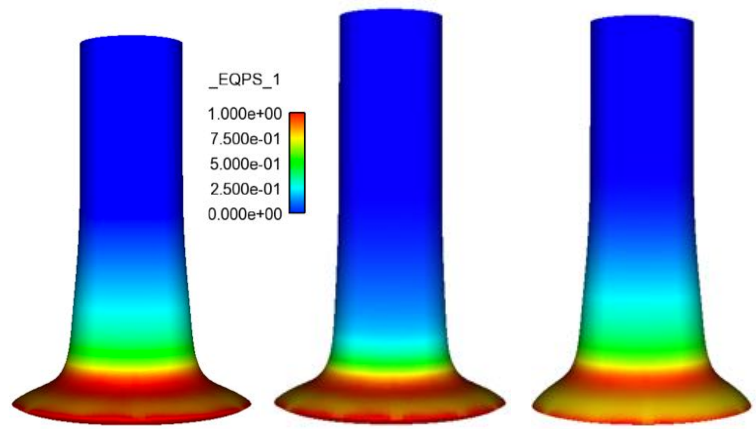

LANL's PTW model | Sandia's PTW model | Sandia's KP model

Taking a “Step Back”:
Simple Tension of Single Crystal Ta

Strain fields: HR-DIC vs. CP-FEM (fixed BC)

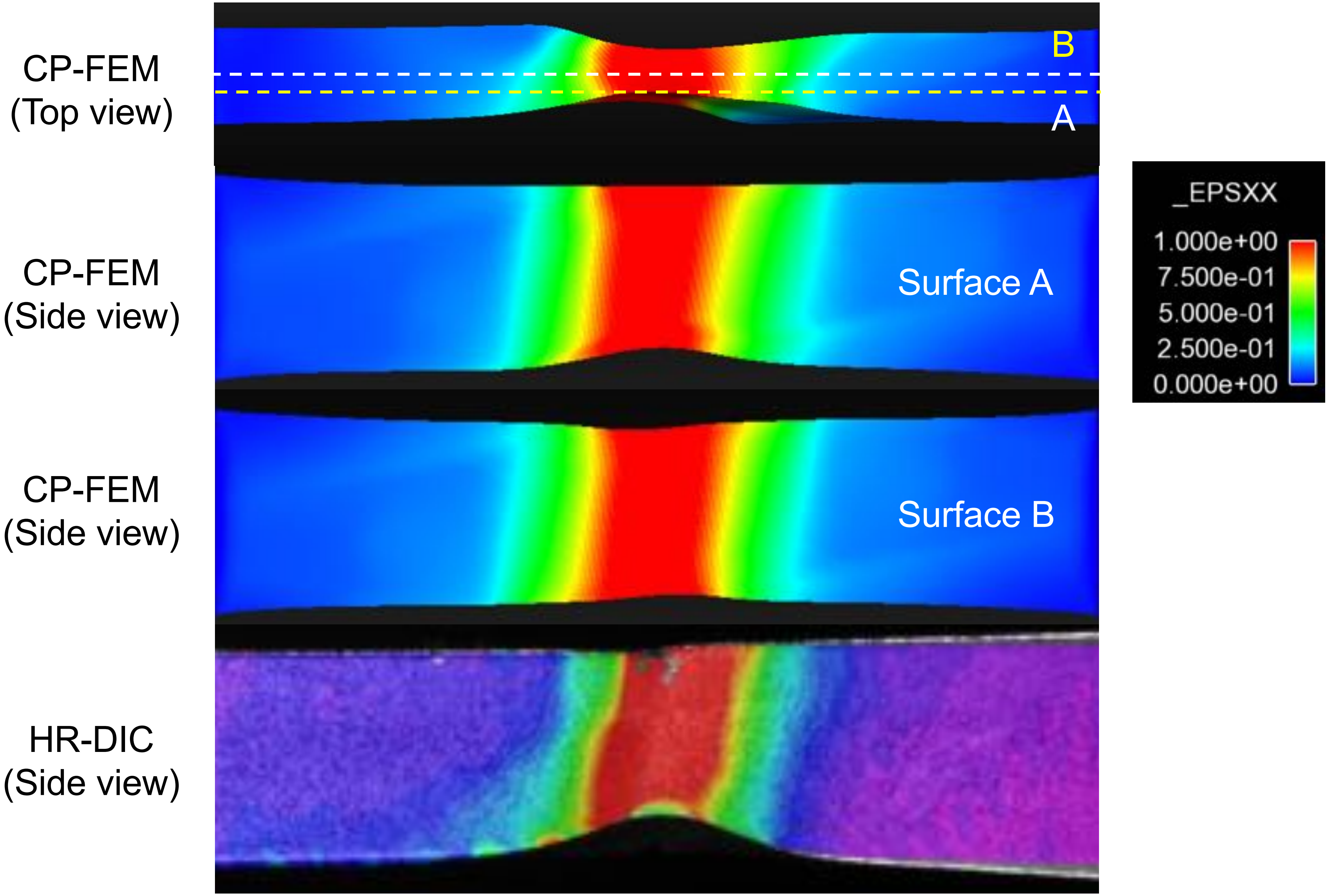

Simulation of Ta single crystal

Ta CP-FEM simulations
Uniaxial tension up to 30%
Strain rate = 2 x 10^{-4} s^{-1}
Euler angles = (94.272°, 35.24°, 308.81°)
Material parameters fit to Ta oligocrystals
1.3×10^{6} hexahedral finite elements (tapered specimen)
No damage

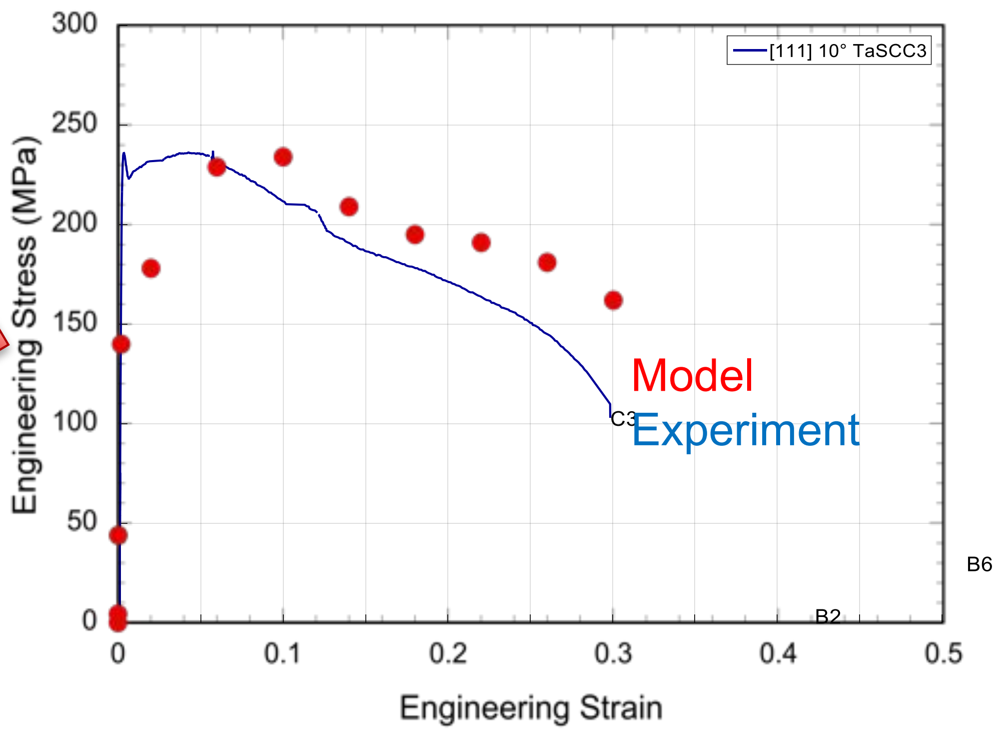

Misorientations

CP-FEM
(Top view)

CP-FEM
(Side view)

CP-FEM
(Side view)

EBSD
(Side view)

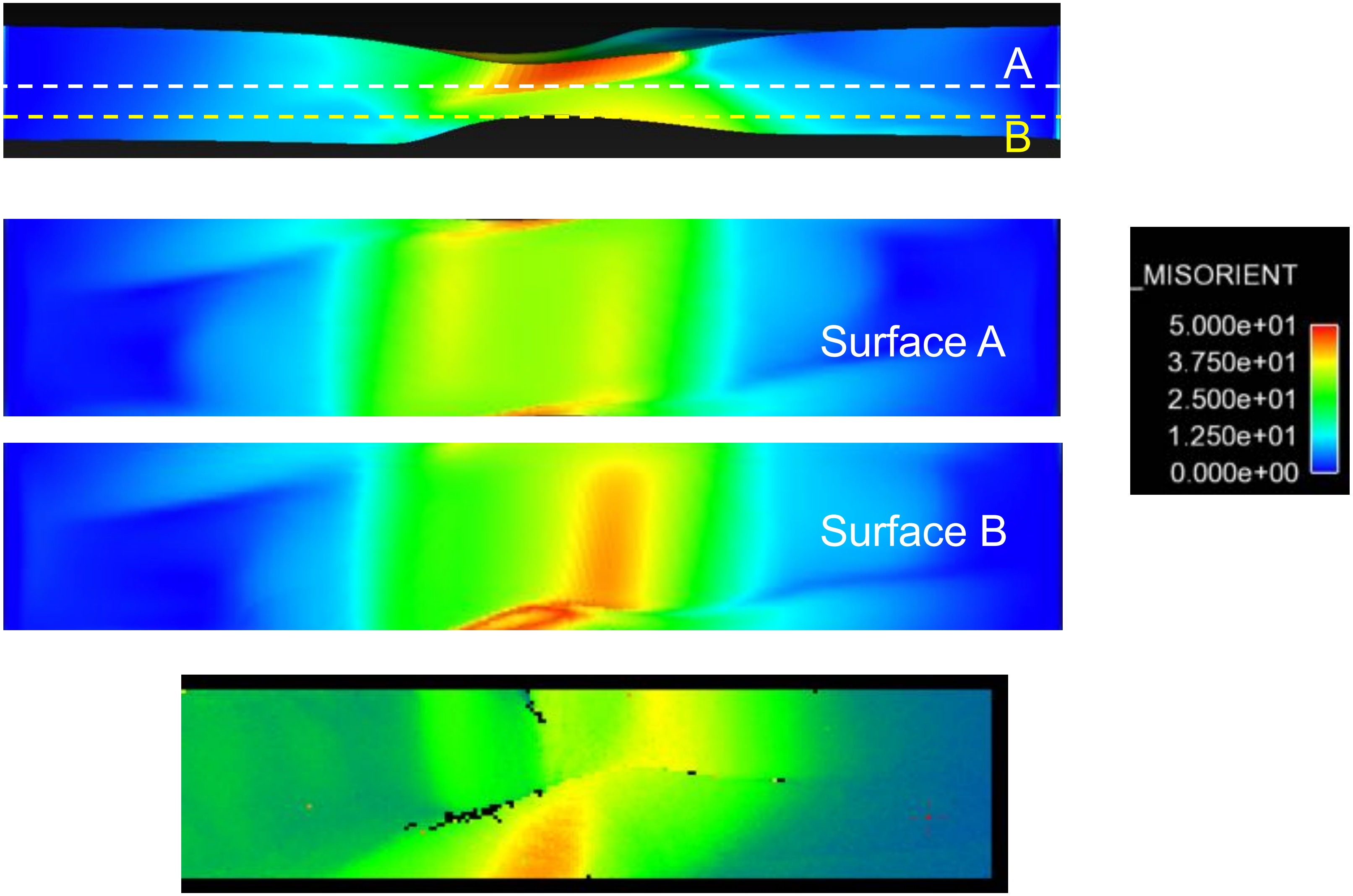

Deformed texture (mid z, fixed BC)

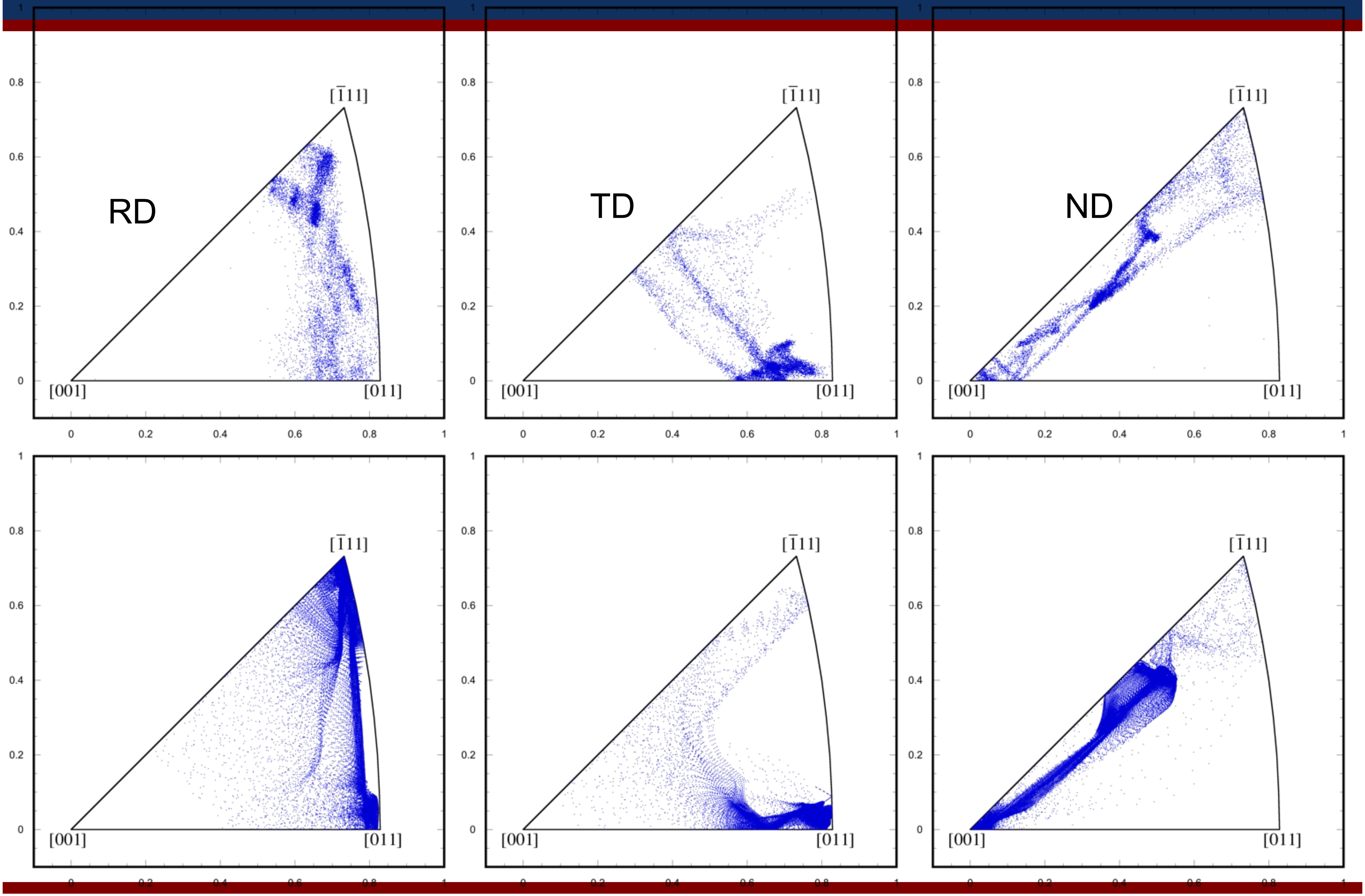

Initial crystal orientations (mid-z plane)

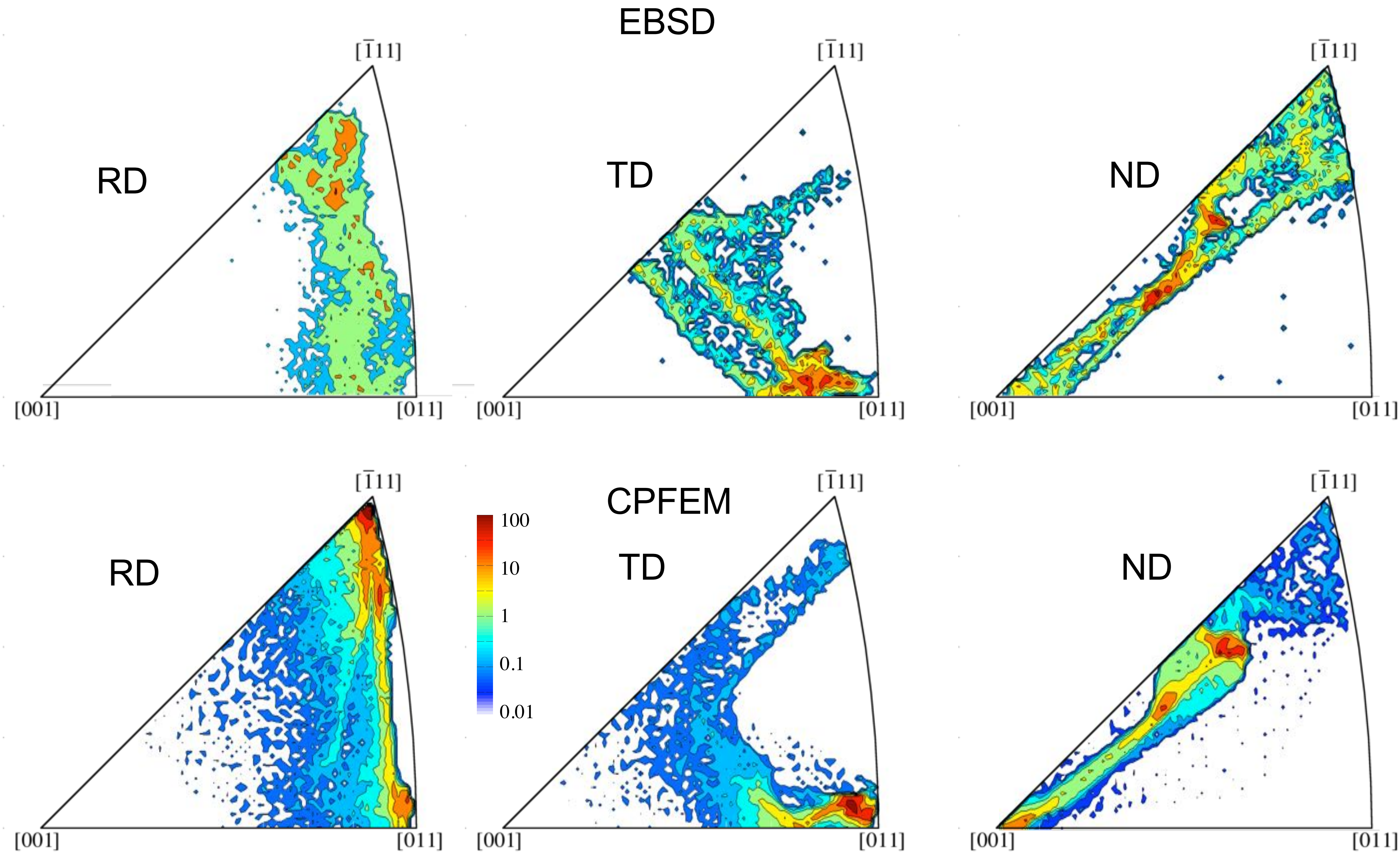

Tensile response

- Dislocation density-based hardening

$$g^{\alpha} = A\mu b\sqrt{\sum_{\beta=1}^{24} \mathbf{H}^{\alpha\beta}\rho^{\beta}} \qquad \dot{\rho}^{\alpha} = \left(\kappa_1\sqrt{\sum_{\beta=1}^{NS} \rho^{\beta}} - \kappa_2\rho^{\alpha}\right)\cdot|\dot{\gamma}^{\alpha}|$$

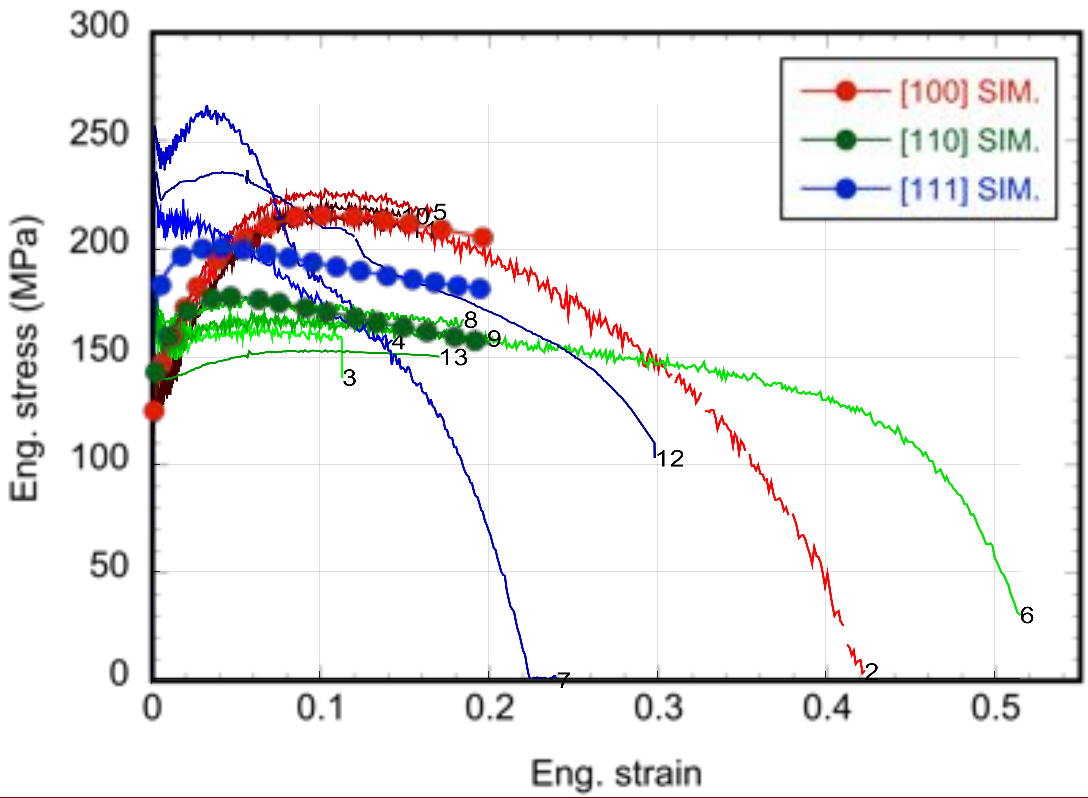

Sandia National Laboratories

Simulated Compression of Single Crystal Ta Cylinders

Biaxial yield surfaces of single crystals

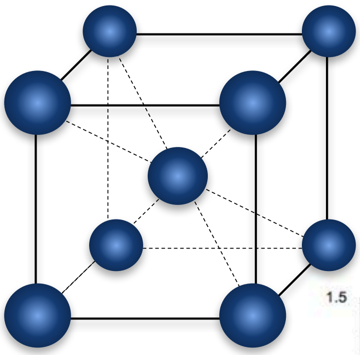

[100] crystal

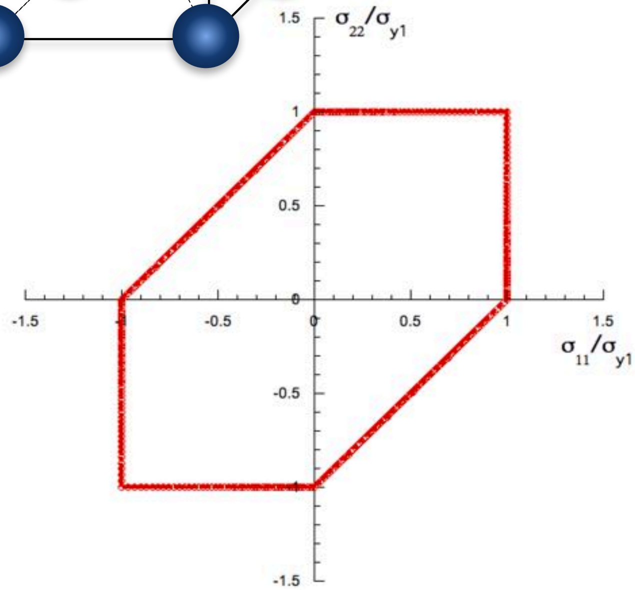

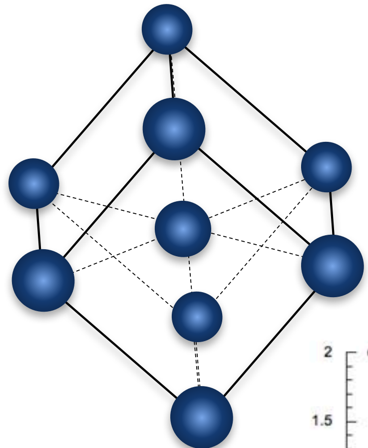

[110] crystal

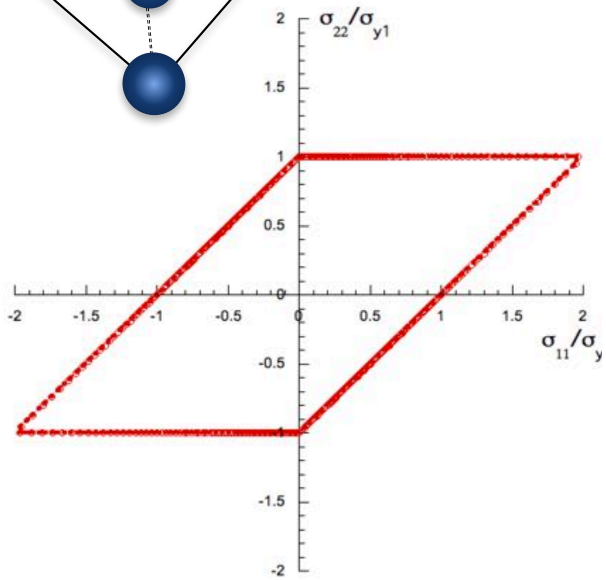

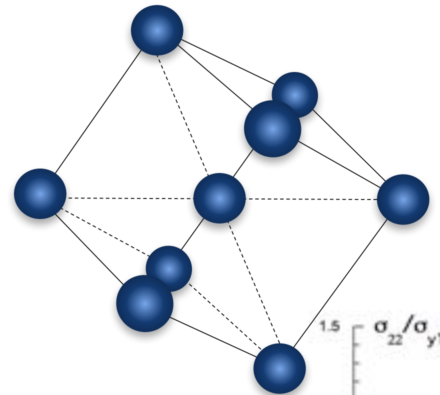

[111] crystal

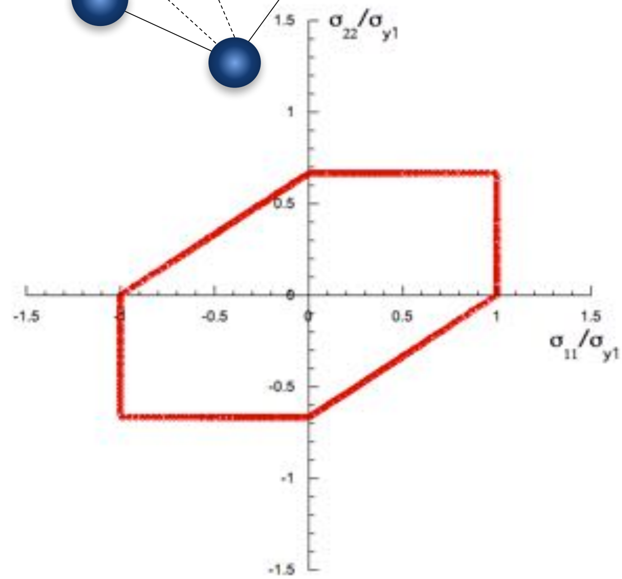

Quasi-static compression of cylinder

30% compression
Strain rate = 10^{-3} s^{-1}

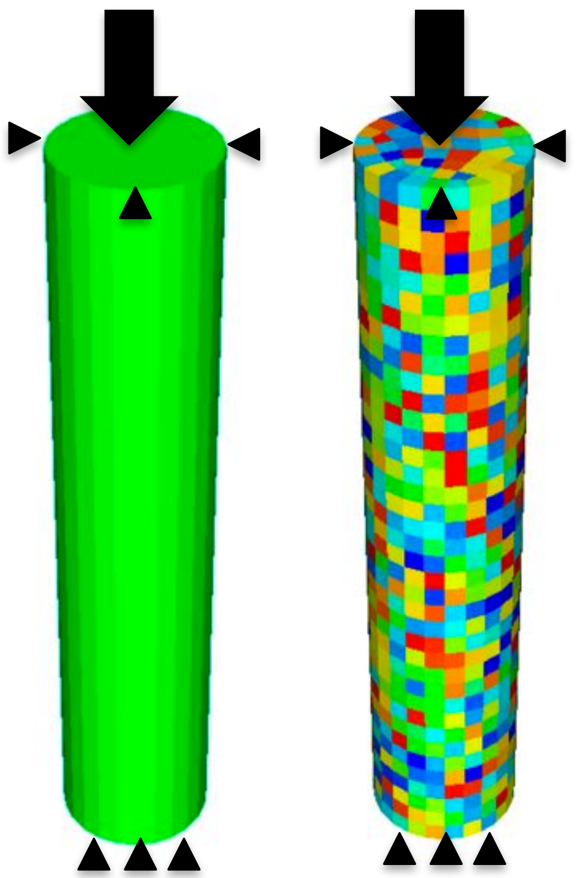

Single Ta Polycrystalline Ta (Starck Ta texture)

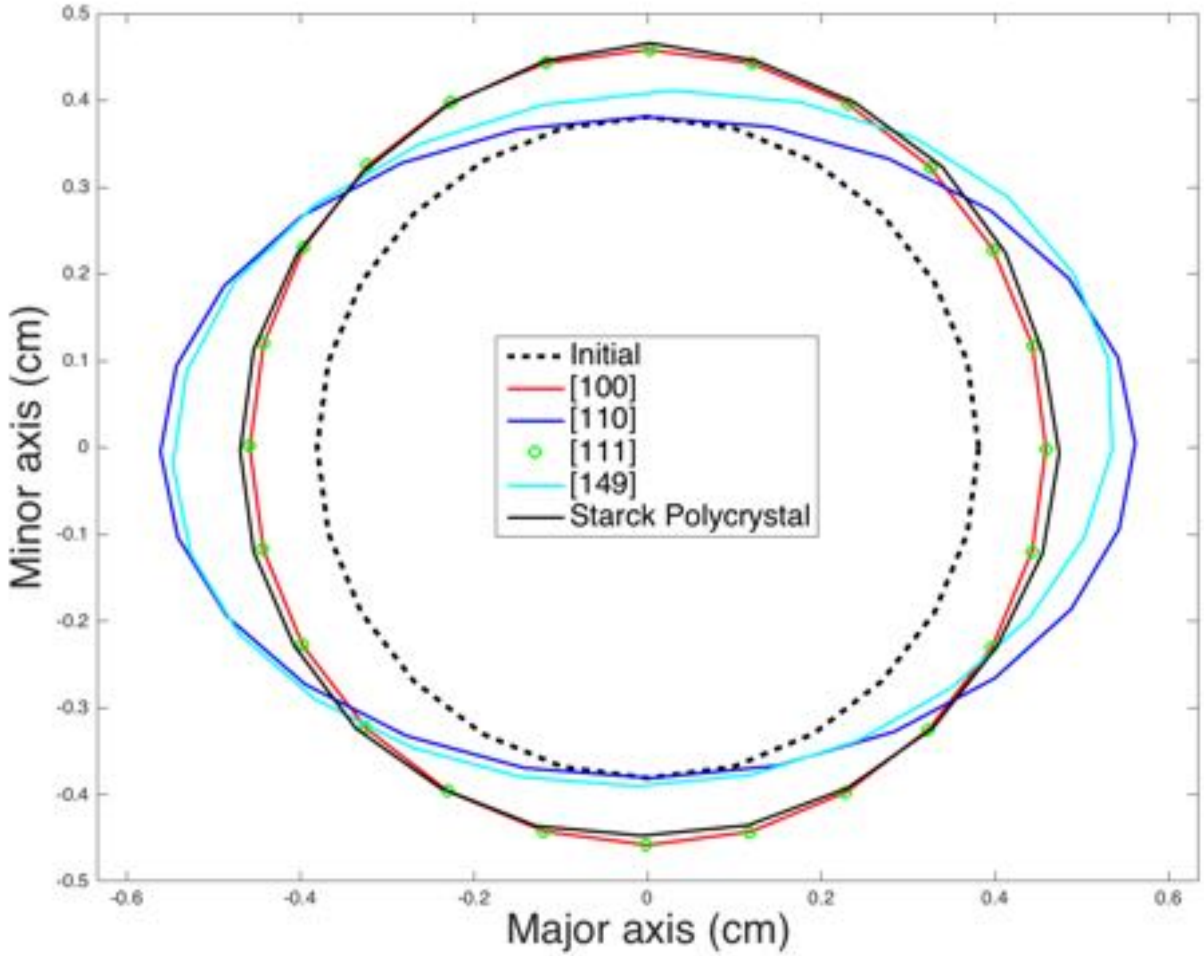

Footprints of single crystals

43 single crystal orientations

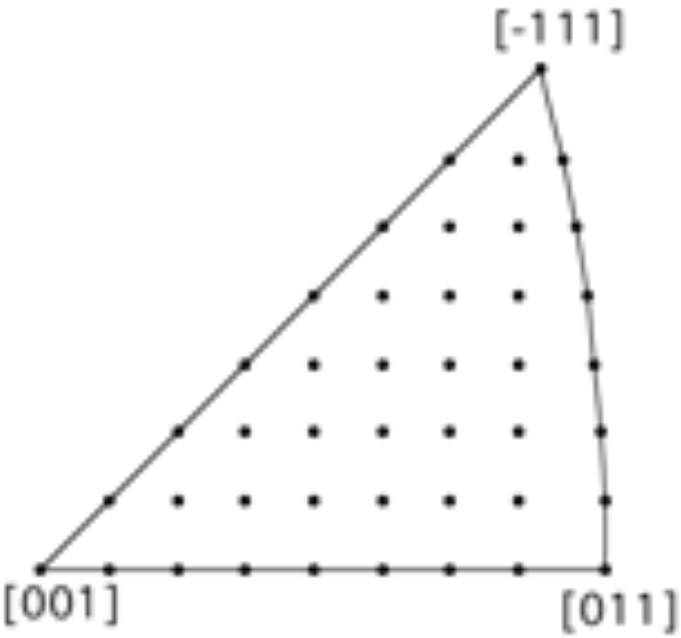

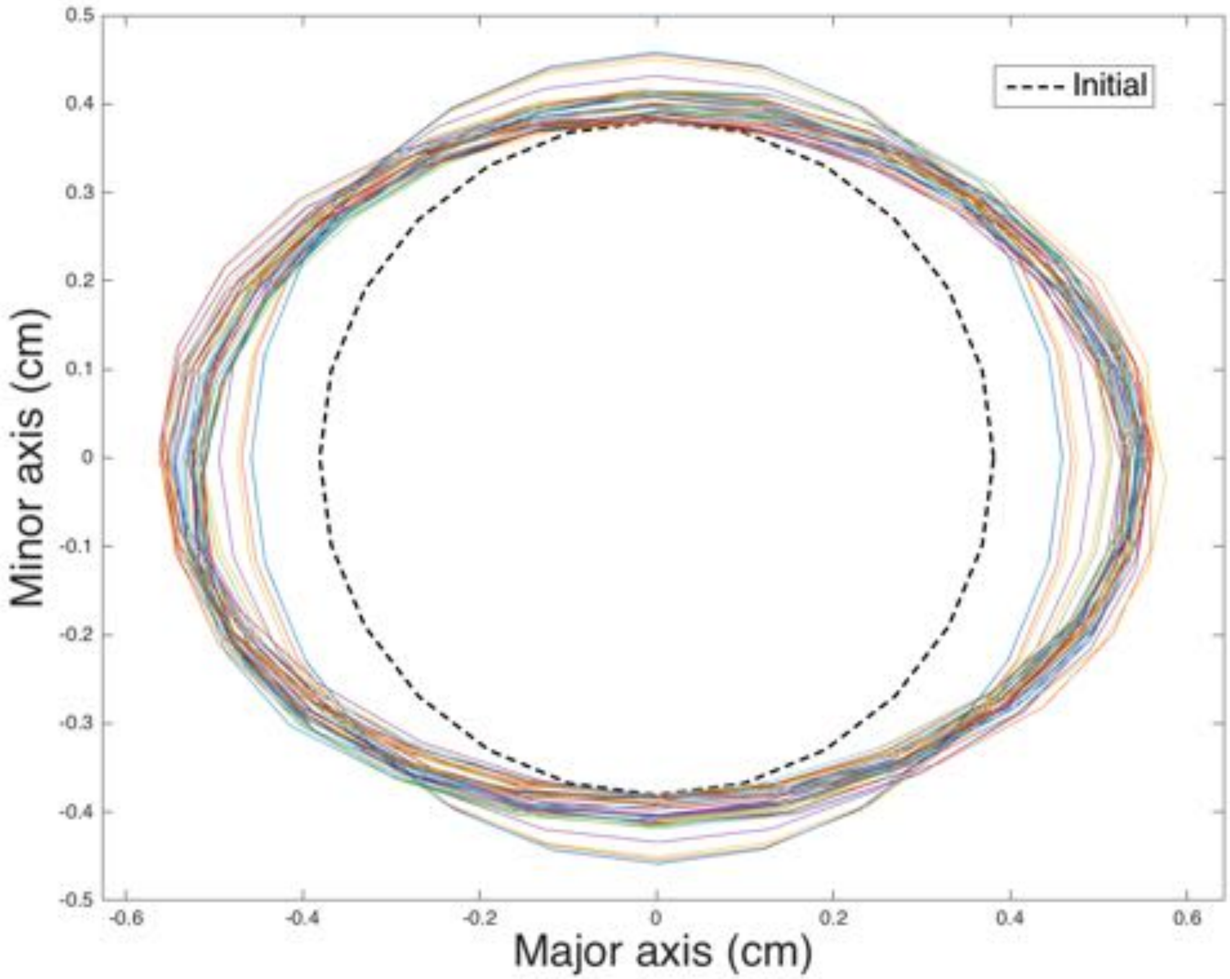

Aspect ratios (=D_{major}/D_{minor})

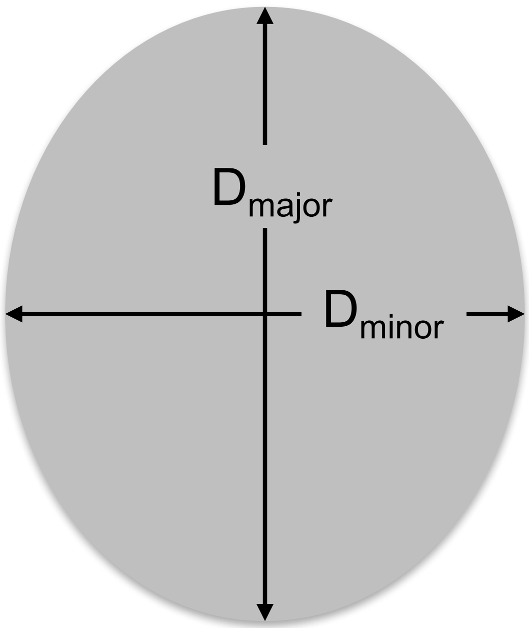

Footprint

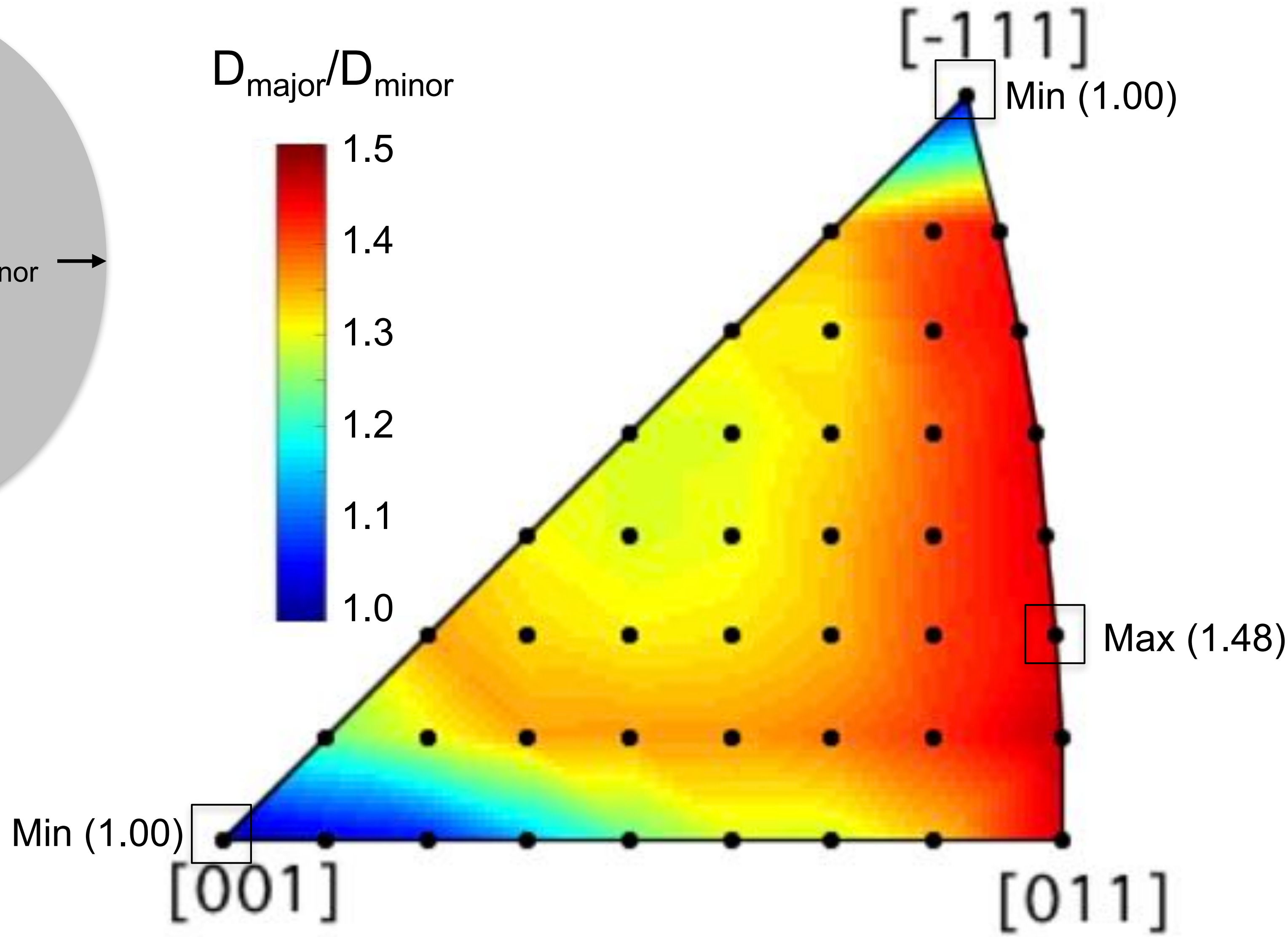

* STARCK polycrystalline Ta : 1.035

Summary

- Developed T and $\dot{\varepsilon}$ dependent flow rule based on dislocation kink-pair theory for Mo, Ta, W and Nb.
- Predicted T and $\dot{\varepsilon}$ dependent σ_y using CP-FEM model agree well with experimental data.
- MTS model accurately reproduced T and $\dot{\varepsilon}$ dependent σ_y of BCC polycrystals.
- CP-FEM predictions of Ta oligocrystals showed good agreement with measured surface strain fields (HR-DIC) and deformed textures (EBSD).
- Proposed computational method provides a convenient and direct link from the fundamental dislocation physics to the continuum-scale plastic deformation of BCC metals at the grain scale.

Supplementary Slides: Validation on Ta Multicrystals

Experimental Setup

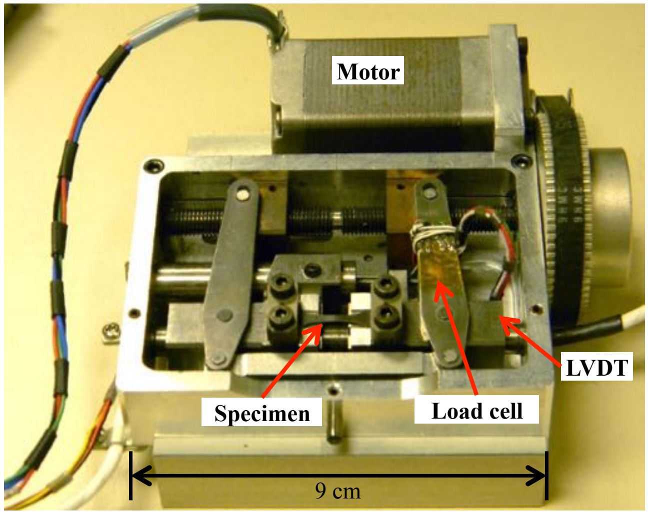

- Tantalum oligocrystals with mostly columnar 2D grain structure eliminate unknown subsurface grain morphology.
- *In-situ* load frame developed at Sandia
- HR-DIC (surface strain fields) and EBSD (crystal orientations) measurements at load inside SEM

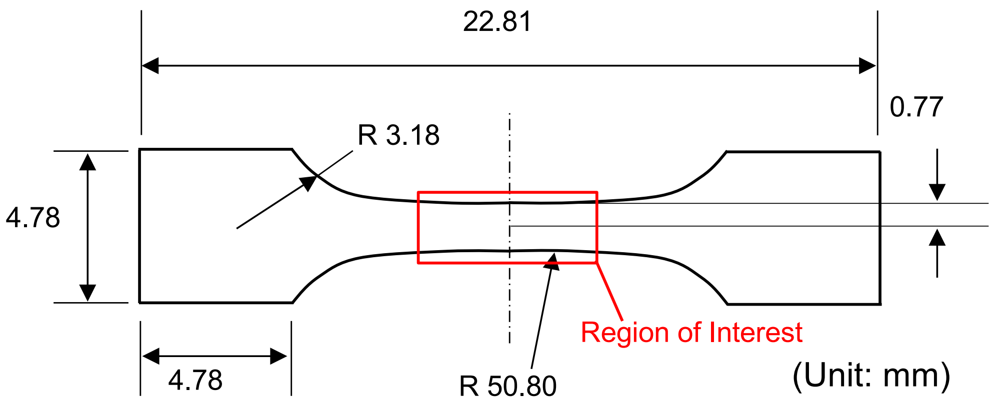

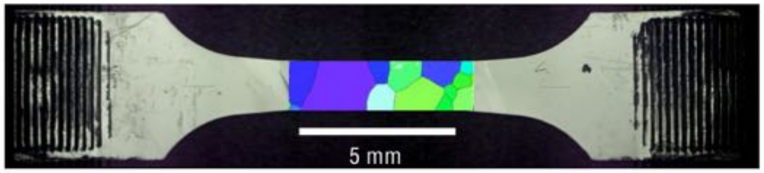

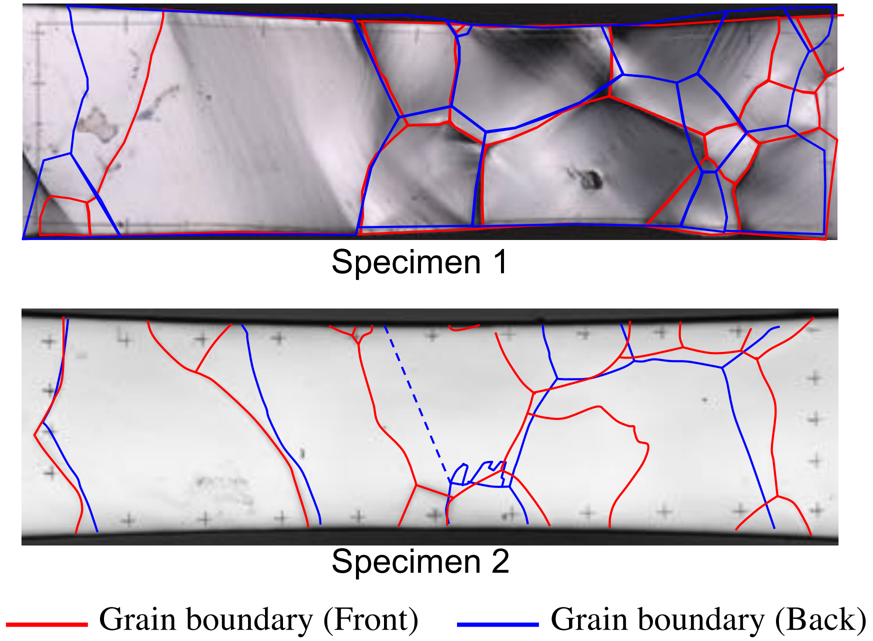

Sandia National Laboratories

Tantalum Oligocrystal Specimens

Specimen 1

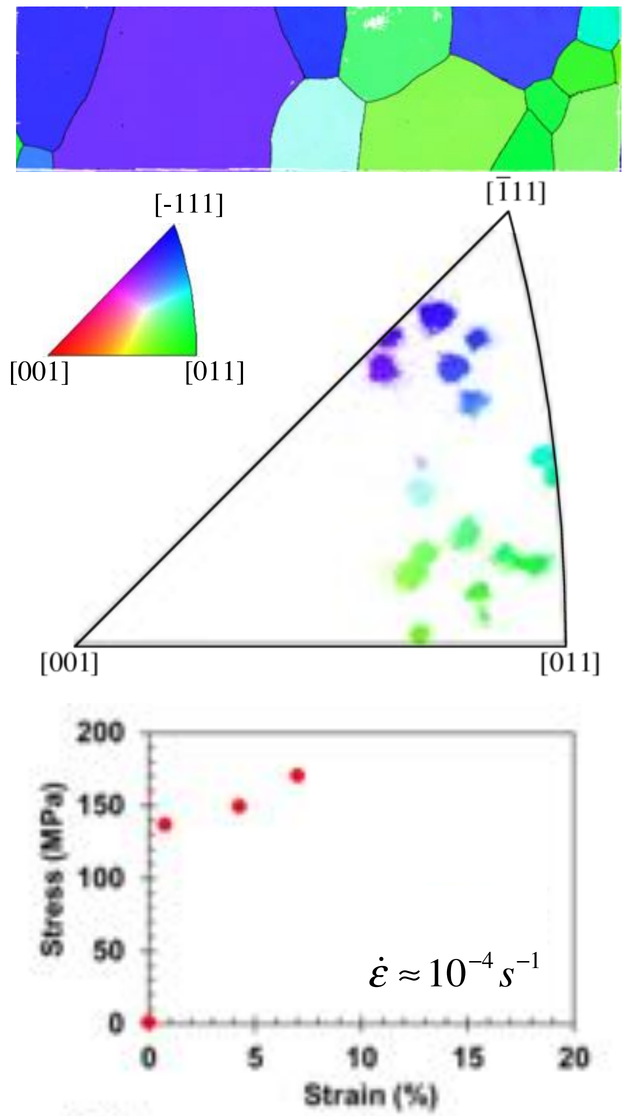

Specimen 2

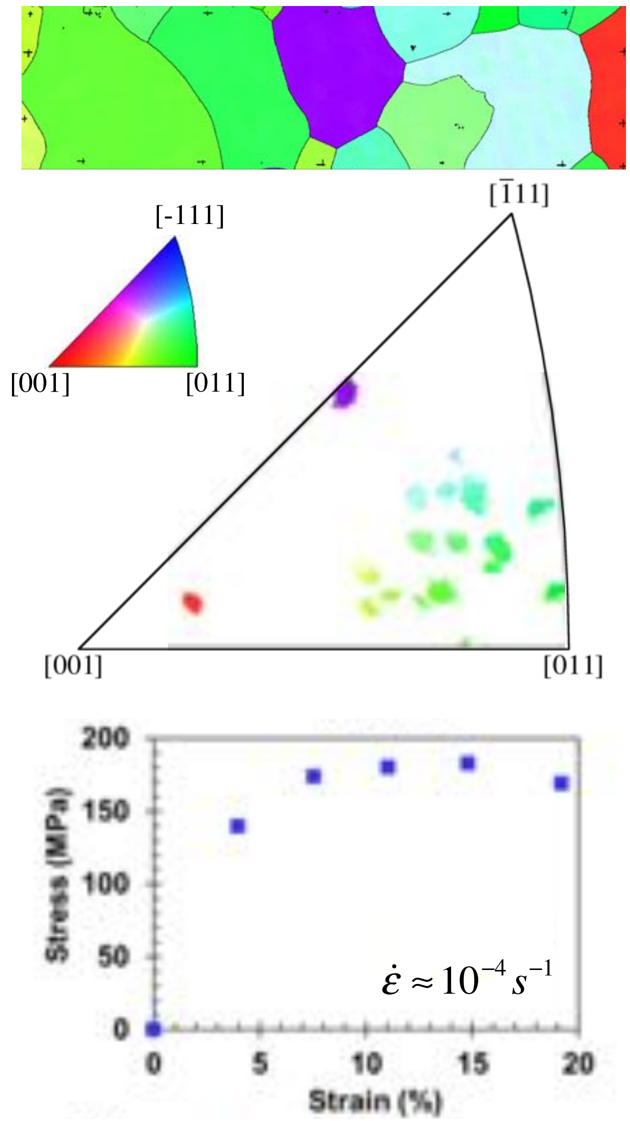

Specimen 3

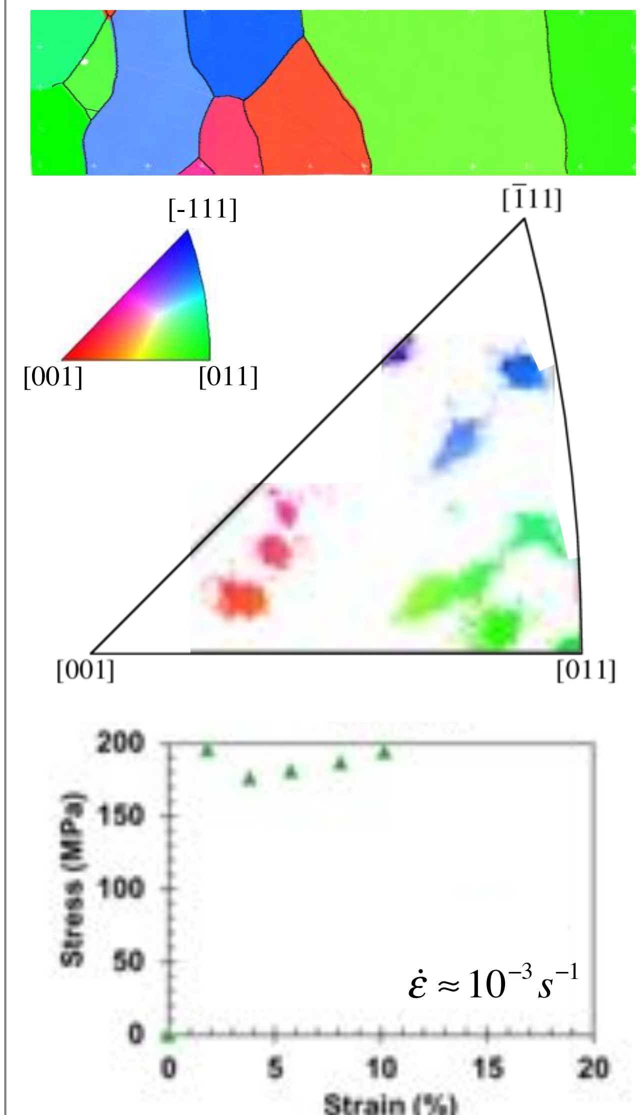

Simulations of Ta Oligocrystals

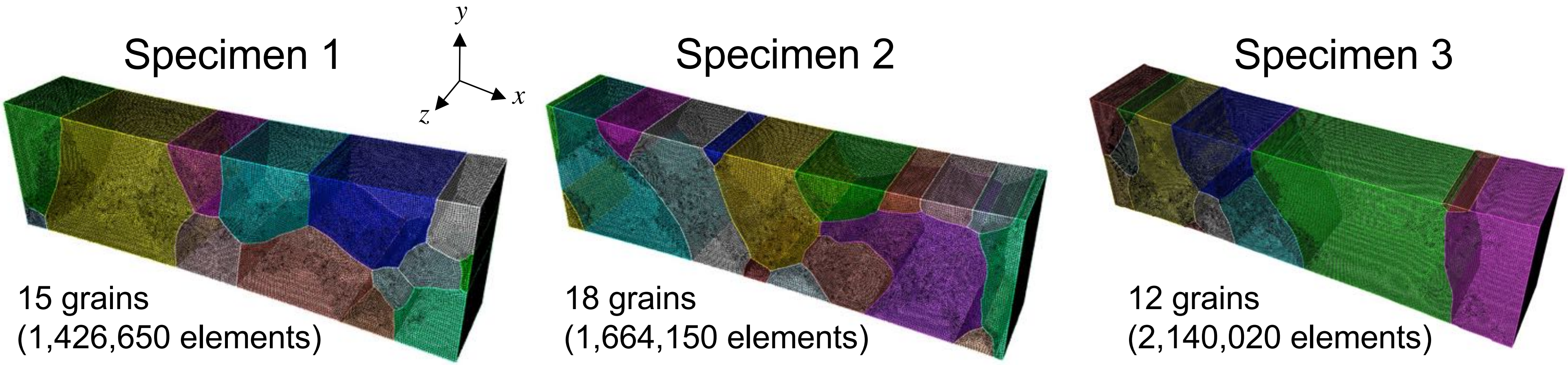

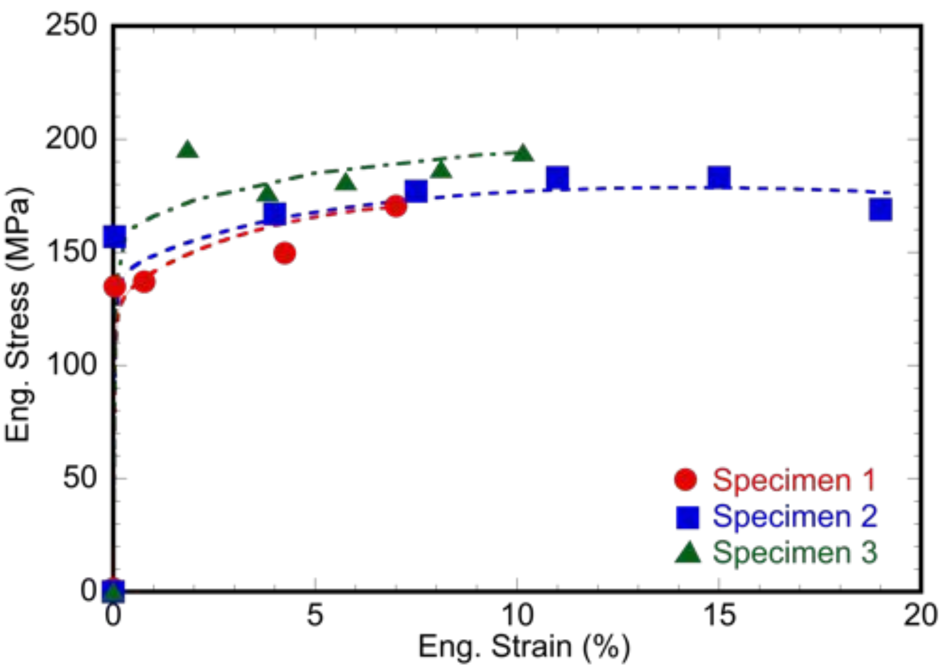

Hardening parameters fit to measured stress-strain data.

$$\tau_{obs}^{\alpha} = A\mu b\sqrt{\sum_{\beta=1}^{NS}\rho^{\beta}} \qquad \dot{\rho}^{\alpha} = \left(\kappa_1\sqrt{\sum_{\beta=1}^{NS}\rho^{\beta}} - \kappa_2\rho^{\alpha}\right)\cdot\left|\dot{\gamma}^{\alpha}\right|$$

$$\tau_{obs,0}(\text{Specimen 1}) = 27MPa$$
$$\tau_{obs,0}(\text{Specimen 2}) = 37MPa$$
$$\tau_{obs,0}(\text{Specimen 3}) = 27MPa$$

$$\kappa_1 = 1.4\times 10^{6}\, m^{-1}$$
$$\kappa_2 = 14$$

"Initial yield" "Hardening shape"

Strain Field Analysis

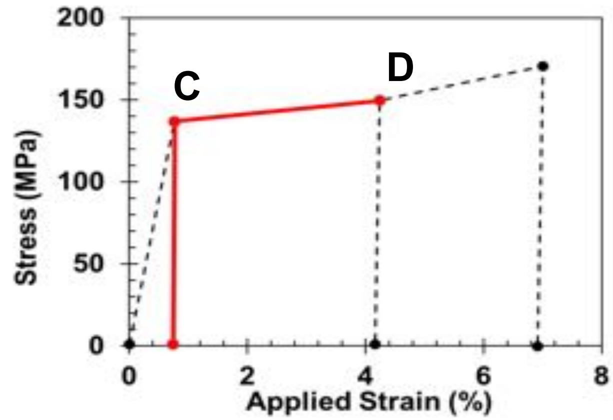

$\Delta\varepsilon_{CD}$ =3.4%

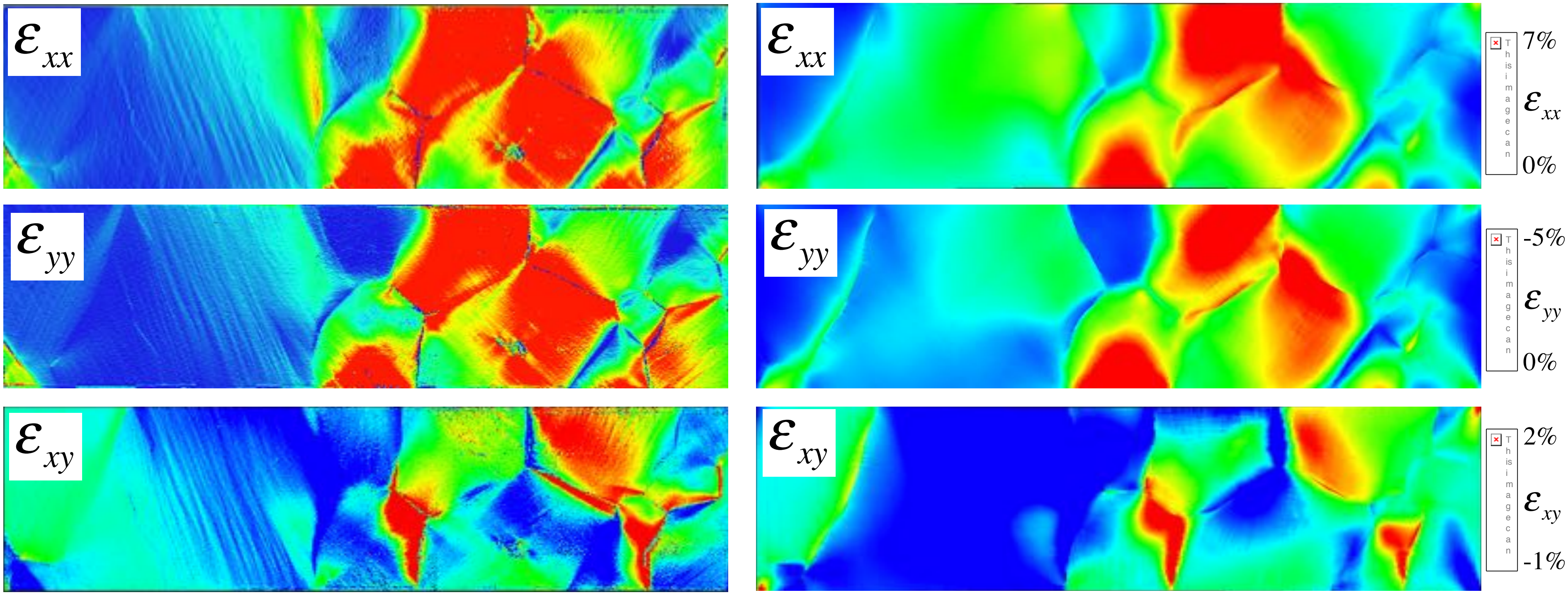

(a) HR-DIC measurements (b) CP-FEM predictions

Measured and predicted strain fields agree well quantitatively.

Texture Predictions

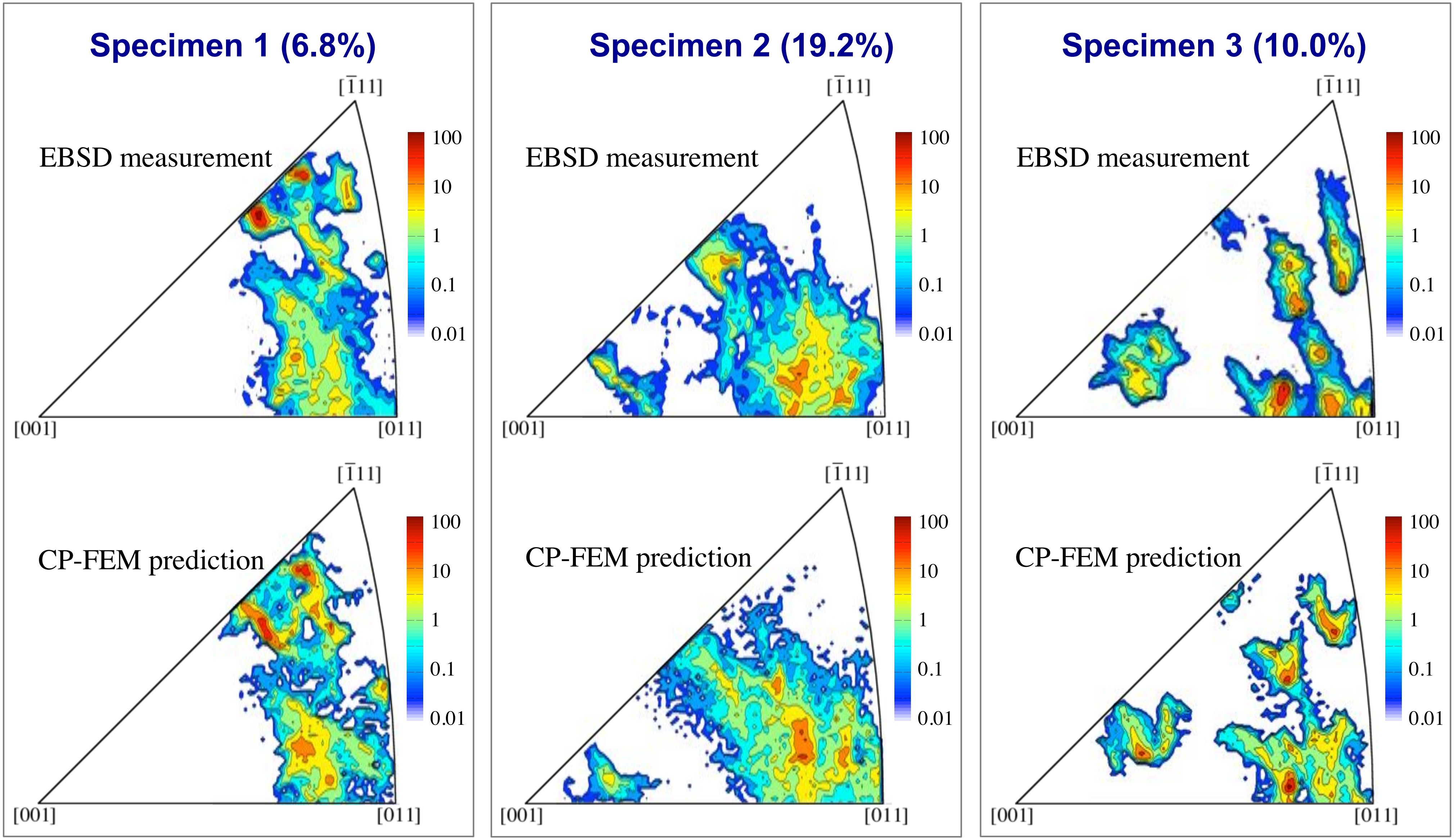

IPF contour plots indicate very good agreement between model and experiment.

Failure Predictions

Ta oligocrystal specimen 2 at 19.2% deformation

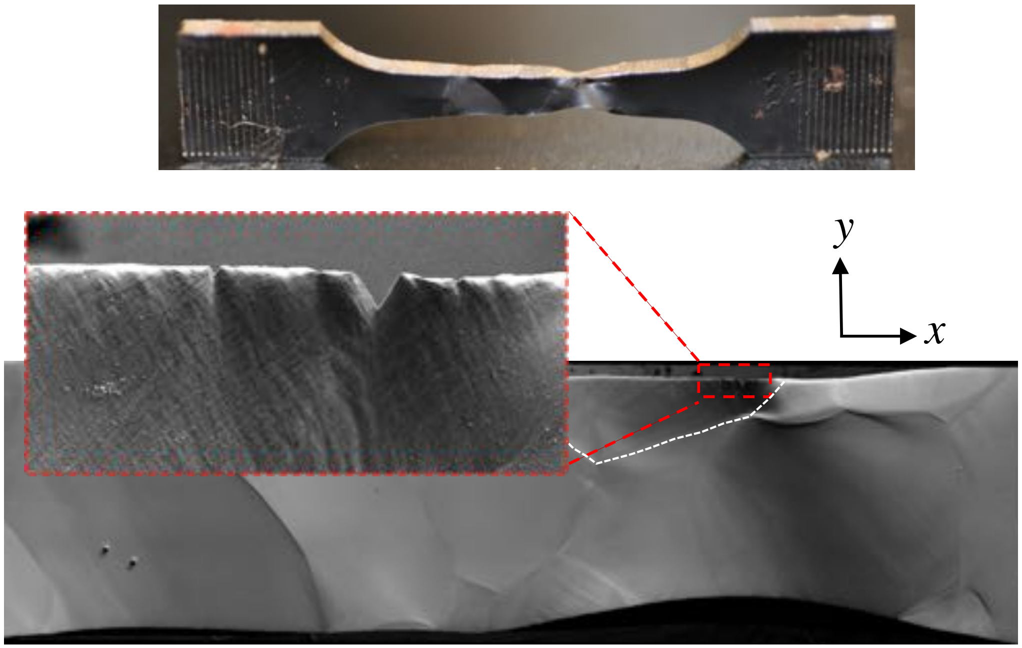

Surface image (side view)

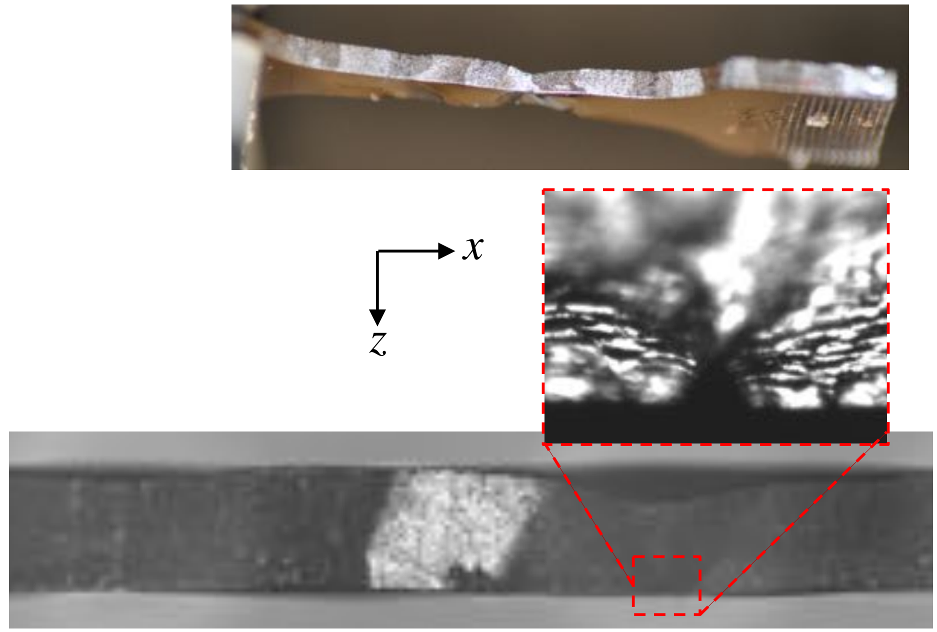

Surface image (top view)

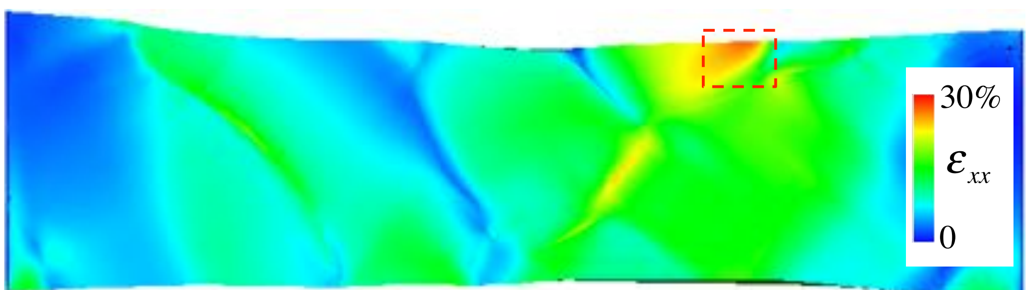

Simulated ε_{xx} (side view)

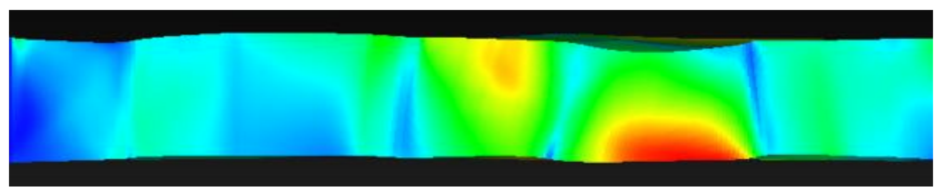

Simulated ε_{xx} (top view)

Failure location agrees with the location of the highest ε_{xx} from the simulation